The Compressible Laminar Boundary Layer on a Yawed Infinite Wing*

L. F. CRABTREE, B.Sc., D.I.C., Grad.R.Ae.S.

Summary: A study of the laminar boundary layer on a yawed infinite wing in a compressible fluid is made. A method is presented for the investigation of compressibility effects by direct solution of the linearised equations of motion, first considerably simplified by the extension of a transformation due to Illingworth and Stewartson, which assumes a heat-insulated surface and a fluid of unit Prandtl number and a coefficient of viscosity which is proportional to the absolute temperature. As an example of this procedure the boundary layer near a stagnation point is calculated. The simplifications necessary for an extension of the momentum method, which is available for a yawed infinite wing in an incompressible fluid, are discussed, and this method is recommended for a first evaluation of the effect of compressibility.

Notation

a velocity of sound

c a constant in equation (8)

d a constant in equation (18)

f Blasius chordwise-flow function (equation (9))

g velocity profile of the spanwise boundary layer (equation (9))

K a constant in equation (21)

l non-dimensional shearing-stress parameter (*see* equations (30) and (34))

$m = -\frac{dU}{dx}\frac{(\theta_x)^2}{\nu}$ = modified Pohlhausen parameter (equation (29))

M Mach number

T absolute temperature

u chordwise velocity component inside the boundary layer

U chordwise velocity component outside the boundary layer

v spanwise velocity component inside the boundary layer

V spanwise velocity component outside the boundary layer

x co-ordinate measured along the surface in the chordwise direction

y co-ordinate measured in the spanwise direction

z co-ordinate measured normal to the surface

---

*Based on part of a thesis presented in partial fulfilment of the requirements for the degree of Ph.D., Cornell University.

Originally received November 1952.

[The Aeronautical Quarterly, Vol. V, July 1954]

γ ratio of specific heats

η a Blasius variable (equation (9))

$\theta_x = \int_0^\infty \frac{\rho u}{\rho_1 U}\left(1-\frac{u}{U}\right)dz$ = momentum thickness of the boundary layer in the chordwise direction

$\theta_y = \int_0^\infty \frac{\rho v}{\rho_1 V}\left(1-\frac{v}{V}\right)dz$ = momentum thickness of the boundary layer in the spanwise direction

$\theta_{xy} = \int_0^\infty \frac{\rho u}{\rho_1 U}\left(1-\frac{v}{V}\right)dz$ = "mixed" momentum thickness of the boundary layer

μ coefficient of viscosity

ν kinematic viscosity

ρ density

$\omega = \frac{1}{2}(\gamma-1)M_r^2$

$\xi = x/c$ (equation (28))

τ shearing stress at the wall

ψ stream function (equations (6) and (9))

Subscripts

$_0$ refers to stagnation conditions

$_1$ refers to conditions at the edge of the boundary layer

$_i$ refers to a related incompressible flow

$_x$ refers to a chordwise component

$_y$ refers to a spanwise component

1. Equations of Motion

For incompressible flow over a yawed infinite wing, the chordwise flow, both inside and outside the boundary layer, is independent of the spanwise flow, as has been shown by Prandtl[3], Jones[4], and Sears[5]. For the same wing in compressible flow, however, Struminsky[6] and Moore[7] have shown that this "independence principle" does not hold (with the exception of isothermal fluids). This may be seen physically, since the temperature affects the chordwise velocity profile by changing the density, and the temperature itself is dependent upon the resultant velocity, *i.e.* upon both the spanwise and chordwise velocity components.

By the use of a transformation of variables and of the velocity distribution outside the boundary layer, due to Illingworth[11] and Stewartson[12], the equations of motion for the two-dimensional compressible boundary layer problem may be reduced exactly to those of a related incompressible flow (*see also* Ref. 1). To obtain this result it is necessary to prescribe a heat-insulated surface and a gas

of Prandtl number unity whose coefficient of viscosity varies directly with the absolute temperature. It is evident, by the reasoning already applied to the question of existence of an independence principle, that the Illingworth-Stewartson transformation will not reduce the boundary layer equations of motion for compressible flow over a yawed infinite wing exactly to an incompressible case. However, since great simplification of the two-dimensional problem was achieved by this transformation, it will be used again here, and at least some advantage may be expected. It will be necessary to prescribe the same restrictions of a heat-insulated wall and a gas of Prandtl number unity and whose viscosity is proportional to the absolute temperature.

The properly extended transformation of Illingworth and Stewartson is applied to the boundary layer equations of motion of a yawed infinite wing in the Appendix. New co-ordinates x_1 and z_1 are introduced according to the equations

$$x_1 = \int_{x_0}^{x} \left(\frac{a_1}{a_0}\right)^{\frac{3\gamma-1}{\gamma-1}} dx \qquad . \quad . \quad . \quad . \quad . \quad (1)$$

$$z_1 = \frac{a_1}{a_0} \int_0^z \frac{\rho}{\rho_0} dz \qquad . \quad . \quad . \quad . \quad . \quad (2)$$

where x is the co-ordinate measured along the surface in the chordwise direction and z is measured normal to the surface. The density ρ and speed of sound a are characterised by subscripts 0 referring to stagnation conditions, or 1 referring to conditions at the edge of the boundary layer. Absence of a subscript indicates ambient conditions inside the boundary layer.

The chordwise component U of the velocity at the edge of the boundary layer is transformed by writing

$$U_1 = \frac{a_0}{a_1} U \qquad . \quad . \quad . \quad . \quad . \quad . \quad (3)$$

Equations (1) to (3) reduce the chordwise and spanwise equations of motion to

$$\nu_0 \frac{\partial^3 \psi}{\partial z_1^3} - \frac{\partial \psi}{\partial z_1} \frac{\partial^2 \psi}{\partial x_1 \partial z_1} + \frac{\partial \psi}{\partial x_1} \frac{\partial^2 \psi}{\partial z_1^2} = -U_1 \frac{dU_1}{dx_1} \left[1 + \frac{\gamma-1}{2} M_r^2 \left\{1 - \left(\frac{v}{V}\right)^2\right\}\right] \qquad (4)$$

and

$$\frac{\partial \psi}{\partial z_1} \frac{\partial v}{\partial x_1} - \frac{\partial v}{\partial z_1} \frac{\partial \psi}{\partial x_1} = \nu_0 \frac{\partial^2 v}{\partial z_1^2} \qquad . \quad . \quad . \quad . \quad . \quad (5)$$

respectively, where the stream function ψ is defined by

$$\left.\begin{aligned} \rho u &= \rho_0 \, \partial\psi/\partial z \\ \rho w &= -\rho_0 \, \partial\psi/\partial x \end{aligned}\right\} . \quad . \quad . \quad . \quad . \quad (6)$$

and

$$M_r^2 = V^2 \Big/ \left(a_0^2 - \frac{\gamma-1}{2} V^2\right) \qquad . \quad . \quad . \quad . \quad (7)$$

i.e. M_Y is the Mach number of the spanwise flow at the edge of the boundary layer with respect to the speed of sound *at a stagnation point of the chordwise flow.*

Except for the last term on the right hand side of equation (4) it is seen that this equation and equation (5) are the equations of motion for a related incompressible flow. Further, the parameter

$$\omega = \frac{\gamma - 1}{2} M_Y^2$$

is independent of the chordwise co-ordinate x, since M_Y is constant, by virtue of equation (7), if V, the spanwise velocity at the edge of the boundary layer, is constant.

We consider it as an extreme case when the Mach number of the spanwise flow component reaches unity, since our treatment cannot take into account shock wave–boundary layer interaction. With this restriction the maximum possible value of ω is 0·2, for air with $\gamma = 1{\cdot}4$, and $M_Y = 1$.

This suggests a linearisation of the problem by a series expansion in powers of the parameter ω.

It must be emphasised at this point that the additional term involving ω in equation (4), the chordwise equation of motion, does not represent the complete effect of the spanwise velocity on the chordwise velocity profile; a part of the compressibility effect of the spanwise on the chordwise velocity is implicit in the remaining terms of the equation. This state of affairs stems from the use of the extended Illingworth-Stewartson transformation, as the ratios ρ/ρ_1 and T/T_1 which are involved are calculated from the *resultant* velocities.

2. Flow Near a Stagnation Point

The situation was investigated for the case where the related incompressible flow is that of flow near a stagnation point, *i.e.*

$$U_1 = cx_1 \qquad . \quad . \quad . \quad . \quad . \quad (8)$$

By utilising a transformation of variables due to Blasius (Ref. 8, p. 139)

$$\left.\begin{aligned} \psi &= (\nu c)^{\frac{1}{2}} x_1 f(\eta) \\ \eta &= \left(\frac{c}{\nu}\right)^{\frac{1}{2}} z_1 \\ v &= V g(\eta) \end{aligned}\right\} \quad . \quad . \quad . \quad . \quad . \quad (9)$$

where V is, of course, constant, equations (4) and (5) reduce to

$$f''' - f'^2 + ff'' = -\left\{1 + \omega\left[1 - \left(\frac{v}{V}\right)^2\right]\right\} \quad . \quad . \quad . \quad (10)$$

with boundary conditions $f(0)=f'(0)=0, \quad f'(\infty)=1,$

and
$$g''+fg'=0 \qquad . \quad . \quad . \quad . \quad . \quad (11)$$

with boundary conditions $g(0)=0, \quad g(\infty)=1.$

In these equations primes denote differentiation with respect to η.

We now expand the functions f and g in series of powers of ω:—

$$f=f_1+\omega f_2+\ldots\ldots \qquad . \quad . \quad . \quad . \quad . \quad (12)$$

$$g=g_1+\omega g_2+\ldots\ldots \qquad . \quad . \quad . \quad . \quad . \quad (13)$$

f_1 is found to satisfy the equation

$$f_1'^2-f_1f_1''=1+f_1''', \qquad . \quad . \quad . \quad . \quad . \quad (14)$$

as given by Blasius and Hiemenz. The solution may be found tabulated in Ref. 9.

Thus f_1 is the same function as in the incompressible case, and if first order terms in ω are neglected, the chordwise flow function *of our transformed system* is independent of the spanwise flow function g.

The equation for f_2 is

$$2f_1'f_2'-f_1f_2''-f_2f_1''-f_2'''=1-g_1^2. \qquad . \quad . \quad (15)$$

Also, g_1 and g_2 satisfy the equations

$$g_1''+f_1g_1'=0 \qquad . \quad . \quad . \quad . \quad . \quad (16)$$

and
$$g_2''+f_2g_1'+f_1g_2'=0 \qquad . \quad . \quad . \quad . \quad . \quad (17)$$

respectively.

Equation (16), together with its boundary conditions $g_1(0)=0$ and $g_1(\infty)=1$, is exactly that given and solved by Sears[5] and Cooke[10]. Its solution is

$$g_1=d\int_0^\eta \exp\left(-\int_0^\eta f_1 d\eta\right)d\eta \qquad . \quad . \quad . \quad (18)$$

with the constant $d=0{\cdot}570$, and has been tabulated by Cooke[10].

With the known values of f_1 and g_1, equation (15) may be integrated numerically for f_2. This has been done by Adams's method and the results are given in Table I. The effect of the first-order correction term ωf_2 on the two-dimensional solution f_1 is shown in Fig. 1 for $\omega=0{\cdot}2$. The corresponding effect on the first derivative of f_1 (or the effect on the velocity) is plotted in Fig. 2. It is seen that the velocity correction term $\omega f_2'$ is small.

KRESGE-HOOKER
WAYNE
UNIVERSITY
SCIENTIFIC LIBRARY

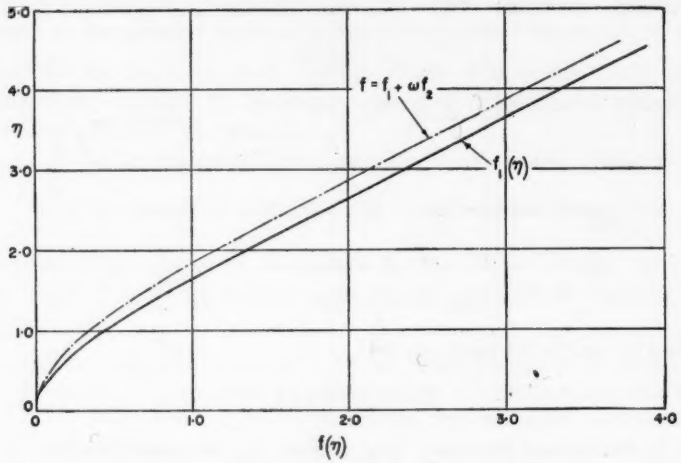

Fig. 1.
Chordwise flow function for stagnation point flow,
$U_1 = cx_1$, with $\omega = 0{\cdot}2$.

These results have been transformed back into the physical plane to give the actual velocity profiles shown in Fig. 3. The use of the Illingworth-Stewartson transformation even at the zero approximation in ω ($f = f_1$) is seen to give a significant improvement over the incompressible assumption for the chordwise velocity profile. The first approximation, $f = f_1 + \omega f_2$ changes the velocity profile further in the same sense.

Now the solution of equation (11) is (18) if f_1 is replaced by $f_1 + \omega f_2$, with the constant d to be evaluated from the boundary condition $g(\infty) = 1$. This numerical quadrature has been carried out (*see* Table I) and the constant is found to be

$$\omega = 0{\cdot}525 \ldots\ldots \qquad (19)$$

for $d = 0{\cdot}2$.

Thus the function g_2 may be calculated without directly solving equation (17), and the solution may be written

$$\omega g_2 = 0{\cdot}525 \int_0^\eta \exp\left(-\int_0^\eta (f_1 + \omega f_2)\, d\eta\right) d\eta - 0{\cdot}570 \int_0^\eta \exp\left(-\int_0^\eta f_1 d\eta\right) d\eta \qquad (20)$$

for $\omega = 0{\cdot}2$, neglecting terms of order ω^2.

The second term on the right hand side of equation (20) is that tabulated by Cooke[10] as $G(Y)$. An examination of Table I reveals that the effect of the

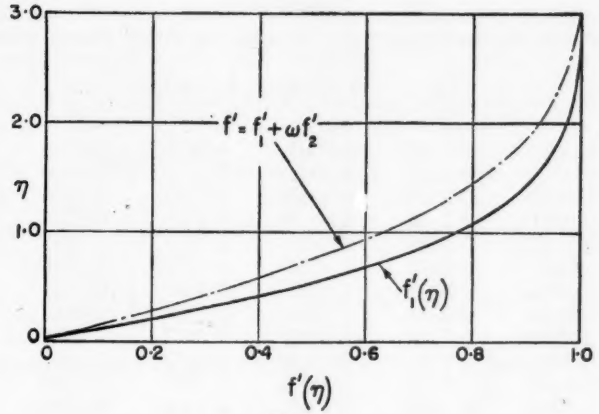

Fig. 2.

Chordwise velocity function for stagnation point flow, $U_1 = cx_1$, with $\omega = 0{\cdot}2$.

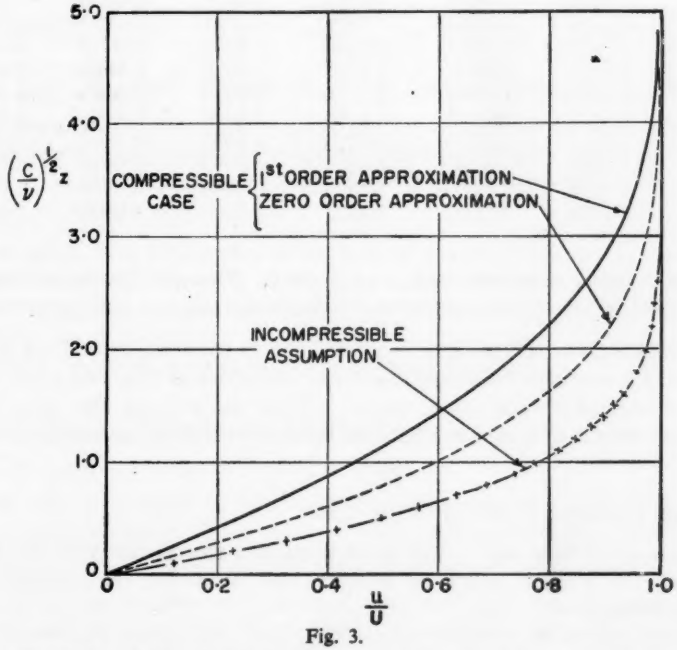

Fig. 3.

Chordwise velocity profiles for stagnation point flow, $U_1 = cx_1$, according to the incompressible assumption, and also the zero and first order approximations to the compressible case, with $\omega = 0{\cdot}2$.

TABLE I

CHORDWISE AND SPANWISE PROFILES (STAGNATION POINT FLOW) WITH $\omega = 0{\cdot}2$

η	f_1	f_1'	$f_1+\omega f_2$	$f_1'+\omega f_2'$	g_1	$g_1+\omega g_2$
0	0	0	0	0	0	0
0·1	0·0060	0·1183	0·0041	0·0811	0·0570	0·0525
0·2	0·0233	0·2266	0·0162	0·1582	0·1140	0·1052
0·3	0·0510	0·3252	0·0357	0·2313	0·1709	0·1575
0·4	0·0881	0·4144	0·0625	0·3005	0·2275	0·2098
0·5	0·1336	0·4946	0·0958	0·3657	0·2835	0·2617
0·6	0·1867	0·5662	0·1355	0·4271	0·3388	0·3131
0·7	0·2466	0·6298	0·1812	0·4847	0·3921	0·3638
0·8	0·3124	0·6859	0·2324	0·5386	0·4461	0·4136
0·9	0·3835	0·7350	0·2888	0·5887	0·4974	0·4622
1·0	0·4592	0·7778	0·3501	0·6352	0·5468	0·5095
1·2	0·6220	0·8467	0·4856	0·7176	0·6387	0·5988
1·4	0·7966	0·8968	0·6362	0·7864	0·7199	0·6798
1·6	0·9798	0·9324	0·7994	0·8425	0·7891	0·7511
1·8	1·1688	0·9569	0·9724	0·8870	0·8461	0·8120
2·0	1·3619	0·9732	1·1533	0·9211	0·8912	0·8621
2·2	1·5577	0·9841	1·3402	0·9469	0·9256	0·9021
2·4	1·7552	0·9905	1·5316	0·9651	0·9508	0·9327
2·6	1·9537	0·9946	1·7259	0·9777	0·9685	0·9552
2·8	2·1529	0·9971	1·9224	0·9865	0·9806	0·9713
3·0	2·3525	0·9985	2·1203	0·9921	0·9884	0·9822
3·2	2·5522	0·9992	2·3190	0·9955	0·9933	0·9894
3·4	2·7521	0·9996	2·5183	0·9975	0·9963	0·9939
3·6	2·9520	0·9998	2·7179	0·9987	0·9981	0·9967
3·8	3·1518	0·9999	2·9175	0·9993	0·9990	0·9983
4·0	3·3518	1·0000	3·1175	0·9997	0·9995	0·9992
4·2	3·5518	1·0000	3·3174	0·9999	0·9998	0·9996
4·4	3·7518	1·0000	3·5174	0·99995	0·9999	0·9999
4·6	3·9518	1·0000	3·7174	1·0000	1·0000	1·0000

first-order velocity correction term, ωg_2, is small. Thus the "universal" spanwise velocity profile[1] is also found for the compressible case, to a good approximation.

Having obtained a first-order approximation to the solution for f, the equations (10) and (11) may now be solved directly by the standard trial and error method. Several numerical integrations to infinity will be required and the value of $f''(0)$ is adjusted after each integration until the boundary condition at infinity is satisfied.

3. The General Falkner-Skan Case

The case of flow near a stagnation point is a special case with $K=1$ of the more general solution given by Falkner and Skan for the two-dimensional incompressible flow

$$U_1 = cx_1^K \quad . \quad . \quad . \quad . \quad . \quad . \quad (21)$$

(*see* Ref. 8, p. 140).

The equations for steady flow in the boundary layer, (4) and (5), are satisfied by putting

$$\psi=(\nu c x_1^{K+1})^{\frac{1}{2}} f(\eta)=(\nu U_1 x_1)^{\frac{1}{2}} f(\eta) \quad . \quad . \quad . \quad . \quad (22)$$

$$\text{where } \eta=\left(\frac{c x_1^{K-1}}{\nu}\right)^{\frac{1}{2}} z_1=\left(\frac{U_1}{\nu x_1}\right)^{\frac{1}{2}} z_1 \quad . \quad . \quad . \quad . \quad (23)$$

With these substitutions equation (4) becomes a differential equation for f,

$$f'''+\left\{1+\omega\left[1-\left(\frac{v}{V}\right)^2\right]\right\} K=Kf'^2-\tfrac{1}{2}(K+1)ff'' \quad . \quad . \quad (24)$$

which may be compared with the equation obtained by Falkner and Skan

$$f'''+K=Kf'^2-\tfrac{1}{2}(K+1)ff'' \quad . \quad . \quad . \quad . \quad (25)$$

The equation of motion for the spanwise flow, (5), may be reduced by the same substitutions together with

$$v=Vg(\eta) \quad . \quad . \quad . \quad . \quad . \quad . \quad (26)$$

and the result is

$$g''+\tfrac{1}{2}(K+1)fg'=0, \quad . \quad . \quad . \quad . \quad . \quad (27)$$

which is exactly the result obtained by Cooke[10] in the incompressible case.

The linearisation procedure adopted for the special case of stagnation point flow in Section 2 may, therefore, be utilised again here, and it seems evident that the compressibility corrections in this general case will have the same order of magnitude as in the special case.

In principle then, the solution of the laminar boundary layer on a yawed wing in a compressible fluid may be obtained by a direct solution of the differential equations of motion, as has been indicated. But generally this method is too complicated, so that it seems desirable to use approximate "momentum" or "Pohlhausen" methods for the boundary layer development.

4. The Use of Momentum Methods

4.1. The isothermal compressible case

If the fluid is assumed to be isothermal the independence principle holds, as has been noted previously. Thus the momentum methods developed in Ref. 1 for the incompressible case may be directly extended to the case of a compressible fluid.

The isothermal assumption is, however, a further approximation, and its effect was investigated by calculating the chordwise characteristics of the boundary layer at whose edge the velocity distribution is given by

$$U=U_0(\xi-\xi^3) \quad . \quad . \quad . \quad . \quad . \quad . \quad (28)$$

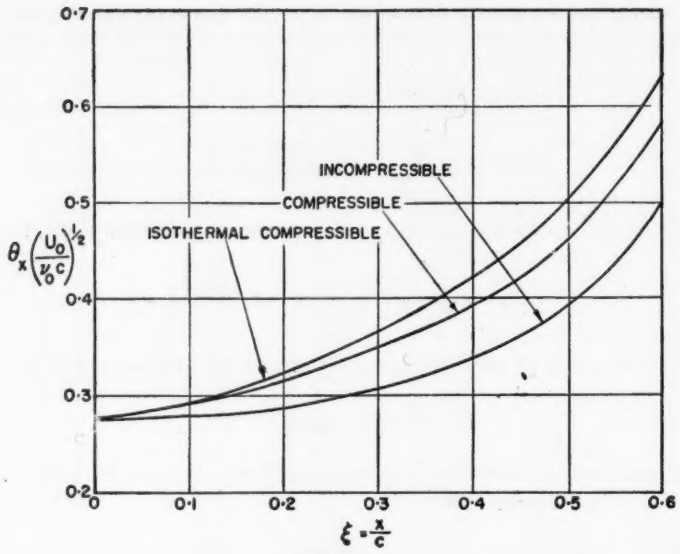

Fig. 4.
Momentum thickness of the laminar boundary layer for the velocity distribution $U=U_0(\xi-\xi^3)$.

representing the flow over a certain class of cylinders, where $\xi=x/c$, c being a typical dimension. The results presented in Ref. 1 are used to calculate the compressible case, and the same results are easily modified to include the additional assumption of an isothermal fluid. The relevant formulae for the limiting case, $\gamma=1$, are[2]

$$\theta_x^2=0{\cdot}45\,\nu_0 \exp(M^2)\; U^{-6}\int_0^x \exp\left(-\frac{M^2}{2}\right)U^5 dx \qquad . \quad . \quad (29)$$

$$m_1=-\frac{dU}{dx}\frac{\theta_x^2}{\nu_0}. \qquad . \quad . \quad . \quad . \quad . \quad . \quad (30)$$

From the values of m_1 given by equation (29) the corresponding values of l_1 are read from the universal curve of Ref. 1. The shear stress at the wall may then be calculated from

$$\tau=l_1\mu_0\frac{U}{\theta_x} \qquad . \quad . \quad . \quad . \quad . \quad . \quad . \quad (31)$$

The values of the momentum thickness θ_x, and of τ, the shear stress at the wall, for the compressible and isothermal compressible cases are plotted in Figs. 4 and 5, in comparison with the incompressible results.

This comparison shows that the isothermal compressible results are closer to the actual compressible values than are the incompressible results.

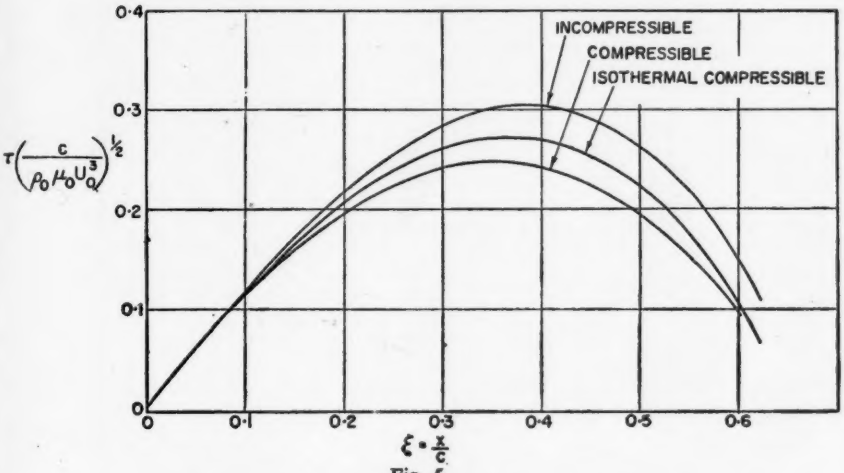

Fig. 5.
Wall shear stress for the velocity distribution $U = U_0(\xi - \xi^3)$.

4.2. *Non-isothermal fluid—further simplifications*

The momentum method may be extended, however, to the case of a non-isothermal fluid, so that although the complete dependence of the chordwise upon the spanwise flow, in the compressible case, is not represented by the method, at least a part of the dependence is accounted for in the solution. This part dependence is obtained by making use of the Illingworth-Stewartson transformation, as explained in Section 1 and, provided that the first order term in ω involving the spanwise velocity profile is neglected, the equation of motion for the chordwise flow is reduced to that of a related incompressible flow.

The results obtained in Part 4 of Ref. 1 for the two-dimensional compressible case may therefore be taken over completely for the calculation of the chordwise characteristics of the boundary layer in the present problem.

The calculation of the spanwise flow in the compressible case requires some further consideration. It may be shown that by use of the extended Illingworth-Stewartson transformation, the spanwise momentum equation reduces to

$$\frac{\partial}{\partial x_1}(U_1\theta_{xy1}) = \frac{\nu_0}{V}\left(\frac{\partial v}{\partial z_1}\right)_{z_1=0} \quad . \quad . \quad . \quad . \quad . \quad (32)$$

This represents the spanwise momentum equation for a possible incompressible flow pattern over a yawed infinite cylinder, and it is therefore reasonable to invoke the aid of the assumptions made for such a case in Ref. 1. Thus, having calculated θ_{x1} and m_1, θ_{y1} (the momentum thickness in the spanwise direction for the related incompressible flow) may be calculated by any of the methods presented therein. The universal spanwise profile then gives v/V directly, and the remaining properties of the boundary layer may be calculated from the following formulae:—

$$\theta_y=\theta_{y1}\left(\frac{T_0}{T_1}\right)^{\frac{\gamma+1}{2(\gamma-1)}} \quad . \quad . \quad . \quad . \quad . \quad . \quad (33)$$

$$\tau_y=\mu_0\left(\frac{\partial v}{\partial z}\right)_{z=0}=\mu_0\left(\frac{\partial v}{\partial z_1}\right)_{z_1=0}\left(\frac{T_1}{T_0}\right)^{\frac{3\gamma-1}{2(\gamma-1)}} \quad . \quad . \quad . \quad . \quad (34)$$

or, since[1]

$$\frac{1}{V}\left(\frac{\partial v}{\partial z_1}\right)_{z_1=0}=\frac{l(m=0)}{\theta_y} \quad . \quad . \quad . \quad . \quad . \quad . \quad (35)$$

and

$$l(m=0)=0{\cdot}225,$$

therefore

$$\tau_y=0{\cdot}225\,\mu_0\frac{V}{\theta_{y1}}\left(\frac{T_1}{T_0}\right)^{\frac{3\gamma-1}{2(\gamma-1)}} \quad . \quad . \quad . \quad . \quad . \quad (36)$$

or

$$\tau_y=0{\cdot}225\,\mu_0\frac{V}{\theta_y}\left(\frac{T_1}{T_0}\right). \quad . \quad . \quad . \quad . \quad (37)$$

Thus, the compressibility effect for yawed wings can partially be taken into account by the momentum method without any essential complication.

Conclusions

In principle, the solution of the laminar boundary layer on a yawed infinite wing in a compressible fluid may be obtained by a direct solution of the linearised differential equations of motion. These equations are first considerably simplified by the extension of a transformation due to Illingworth and Stewartson which entails the assumptions of a heat-insulated surface and a fluid of unit Prandtl number and a coefficient of viscosity which is proportional to the absolute temperature. Even so, this method is generally too complicated, and therefore the use of an approximate momentum method is considered for the boundary layer development.

First, the further assumption of an isothermal fluid allows of the direct extension of the momentum method which is available for incompressible flow.

Secondly, the linearisation procedure is used to extend this method to the case of a non-isothermal fluid. The momentum method may thus be used to account partially for the compressibility effect on yawed wings without any essential complication.

Acknowledgment

The author wishes to acknowledge with gratitude the constant encouragement and advice afforded him throughout this work by Nicholas Rott, Associate Professor, and Professor William R. Sears, Director, of the Graduate School of Aeronautical Engineering, Cornell University.

REFERENCES

1. ROTT, N. and CRABTREE, L. F. (1952). Simplified Laminar Boundary Layer Calculations for Bodies of Revolution and for Yawed Wings. *Journal of the Aeronautical Sciences*, Vol. 19, pp. 553-565, 1952.
2. CRABTREE, L. F. (1952). The Laminar Boundary Layer on a Yawed Infinite Cylinder. Thesis, Cornell University, September 1952.
3. PRANDTL, L. (1946). Ueber Reibungsschichten bei dreidimensionalen Strömungen. British M.A.P. Volkenrode Report and Translation No. 64, 1946.
4. JONES, R. T. (1947). Effects of Sweep-back on Boundary Layer and Separation. N.A.C.A. T.N. 1402 (1947), and N.A.C.A. Report 884 (1949).
5. SEARS, W. R. (1948). The Boundary Layer of Yawed Cylinders. *Journal of the Aeronautical Sciences*, Vol. 15, pp. 49-52, 1948.
6. STRUMINSKY, V. V. (1946). Sideslip in a Viscous Compressible Gas. Dokl. Akad. Nauk., SSSR. T.54, 1946 (also N.A.C.A. T.M. 1276).
7. MOORE, F. K. (1951). Three-dimensional Compressible Laminar Boundary Layer Flow. N.A.C.A. T.N. 2279, 1951.
8. GOLDSTEIN, S. (editor) (1938). *Modern Developments in Fluid Dynamics*, Vol. 1, Oxford, 1938.
9. HOWARTH, L. (1934). Steady Flow in the Boundary Layer near the Surface of a Cylinder in a Stream. R. & M. 1632, 1934.
10. COOKE, J. C. (1950). The Boundary Layer of a Class of Infinite Yawed Cylinders. *Proc. Camb. Phil. Soc.*, Vol. 46, pp. 645-648, 1950.
11. ILLINGWORTH, C. R. (1949). Steady Flow in the Laminar Boundary Layer of a Gas. *Proc. Roy. Soc.*, Vol. 199, pp. 533-558. 1949.
12. STEWARTSON, K. (1949). Correlated Incompressible and Compressible Boundary Layers. *Proc. Roy. Soc.*, Vol. 200, pp. 84-100, 1949.

APPENDIX

TRANSFORMATION OF THE BOUNDARY LAYER EQUATIONS OF A YAWED INFINITE WING IN A COMPRESSIBLE FLUID

Using the co-ordinate system defined in Section 1, the equations of motion for steady flow are

$$u\frac{\partial u}{\partial x}+w\frac{\partial u}{\partial z}=-\frac{1}{\rho}\frac{\partial p}{\partial x}+\frac{1}{\rho}\frac{\partial}{\partial z}\left(\mu\frac{\partial u}{\partial z}\right). \quad . \quad . \quad . \quad . \quad (38)$$

$$u\frac{\partial v}{\partial x}+w\frac{\partial v}{\partial z}=\frac{1}{\rho}\frac{\partial}{\partial z}\left(\mu\frac{\partial v}{\partial z}\right). \quad . \quad . \quad . \quad . \quad (39)$$

$$0=\frac{\partial p}{\partial z} \quad . \quad . \quad . \quad . \quad . \quad . \quad . \quad . \quad (40)$$

together with the equation of continuity

$$\frac{\partial x}{\partial}(\rho u)+\frac{\partial}{\partial z}(\rho w)=0. \quad . \quad . \quad . \quad . \quad . \quad . \quad . \quad . \quad (41)$$

The equation expressing conservation of energy is

$$\rho\left(u\frac{\partial}{\partial x}+w\frac{\partial}{\partial z}\right)\left(\frac{u^2+v^2}{2}+C_pT\right)=\frac{\partial}{\partial z}\mu\frac{\partial}{\partial z}\left(\frac{u^2+v^2}{2}+C_pT\right) \quad . \quad (42)$$

for a Prandtl number of unity.

If there is no heat transfer between the gas and the wing surface, the simple integral of equation (42) may be used,

$$C_pT+\frac{u^2+v^2}{2}=\text{constant}. \quad . \quad . \quad . \quad . \quad (43)$$

The Illingworth-Stewartson transformation is[1]

$$\left.\begin{aligned} z_1&=\frac{a_1}{a_0}\int_0^z\frac{\rho}{\rho_0}\,dz \\ x_1&=\int_0^x\left(\frac{a_1}{a_0}\right)^{\frac{3\gamma-1}{\gamma-1}}dx \\ U_1&=\frac{a_0}{a_1}U \end{aligned}\right\} . \quad . \quad . \quad . \quad (44)$$

Note that $V'^2=U^2+V^2$,

where V' = the resultant velocity at the edge of the boundary layer.

Equation (41) implies the existence of a stream function ψ such that

$$\left.\begin{aligned} \rho u&=\rho_0\frac{\partial\psi}{\partial z} \\ \rho w&=-\rho_0\frac{\partial\psi}{\partial x} \end{aligned}\right\} . \quad . \quad . \quad . \quad . \quad . \quad (45)$$

Assuming further that $$\frac{\mu}{\mu_0}=\frac{T}{T_0} \quad . \quad . \quad . \quad . \quad . \quad . \quad (46)$$

i.e. the coefficient of viscosity is directly proportional to the absolute temperature, and substituting from the preceding equations into equation (38), gives

$$\frac{a_1^2}{a_0^2}\left[\frac{\partial\psi}{\partial z_1}\frac{\partial^2\psi}{\partial x\partial z_1}-\frac{\partial\psi}{\partial x}\frac{\partial^2\psi}{\partial z_1^2}\right]+\left(\frac{\partial\psi}{\partial z_1}\right)^2\frac{\gamma-1}{2\rho_1a_0^2}\frac{dx}{dp_1}=-\frac{1}{\rho}\frac{dp}{dx}+\nu_0\frac{p_1}{p_0}\frac{a_1^3}{a_0^3}\frac{\partial^3\psi}{\partial z_1^3} \quad (47)$$

Now $$\frac{\rho_1}{\rho}=\frac{T}{T_1}=1+\frac{\gamma-1}{2}\left[(U^2+V^2)-(u^2+v^2)\right] \quad . \quad . \quad . \quad (48)$$

and $$\frac{p}{p_0}=\frac{p_1}{p_0}=\left(\frac{a_1}{a_0}\right)^{\frac{2\gamma}{\gamma-1}} \quad . \quad . \quad . \quad . \quad . \quad (49)$$

so that equation (47) becomes

$$\nu_0\frac{\partial^3\psi}{\partial z_1^3}-\frac{p_0}{p_1}\frac{a_0}{a_1}\left[\frac{\partial\psi}{\partial z_1}\frac{\partial^2\psi}{\partial x\partial z_1}-\frac{\partial\psi}{\partial x}\frac{\partial^2\psi}{\partial z_1^2}\right]=\left(\frac{a_0}{a_1}\right)^3\frac{p_0}{p_1}\frac{1}{\rho_1}\frac{dp_1}{dx}\left[1+\frac{\gamma-1}{2a_1^2}(U^2+V^2-v^2)\right].$$

Therefore

$$\nu_0 \frac{\partial^3\psi}{\partial z_1^3} - \frac{\partial\psi}{\partial z_1}\frac{\partial^2\psi}{\partial x_1 \partial z_1} + \frac{\partial\psi}{\partial x_1}\frac{\partial^2\psi}{\partial z_1^2} = \left(\frac{a_0}{a_1}\right)^{\frac{5\gamma-3}{\gamma-1}} \frac{1}{\rho_1}\frac{dp_1}{dx}\left[1+\frac{\gamma-1}{2a_1^2}(U^2+V^2-v^2)\right] \quad (50)$$

Now $U_1=(a_0/a_1)U$, from equations (44).

Therefore

$$\frac{dU_1}{dx_1} = \left(\frac{a_0}{a_1}\right)^{\frac{4\gamma-2}{\gamma-1}}\left[1+\frac{\gamma-1}{2}\frac{U^2}{a_1^2}\right]\frac{dU}{dx}$$

and

$$-U_1\frac{dU_1}{dx_1} = \left(\frac{a_0}{a_1}\right)^{\frac{5\gamma-3}{\gamma-1}}\frac{1}{\rho_1}\frac{dp_1}{dx}\left[1+\frac{\gamma-1}{2a_1^2}U^2\right] \quad . \quad . \quad . \quad (51)$$

since for $V'^2=U^2+V^2$ with constant V, then $V'\,dV'/dx,=U\,dU/dx$, and substitution into the right hand side of equation (50) gives

$$\nu_0\frac{\partial^3\psi}{\partial z_1^3} - \frac{\partial\psi}{\partial z_1}\frac{\partial^2\psi}{\partial x_1\partial z_1} + \frac{\partial\psi}{\partial x_1}\frac{\partial^2\psi}{\partial z_1^2} = -U_1\frac{dU_1}{dx_1}\left[1+\frac{\gamma-1}{2}M_V^2\left\{1-\left(\frac{v}{V}\right)^2\right\}\right]. \quad (52)$$

where

$$M_V^2 = V^2/(a_0^2-\tfrac{1}{2}(\gamma-1)V^2),$$

i.e. M_V is the Mach number of the spanwise flow at the edge of the boundary layer with respect to the speed of sound at a stagnation point of the chordwise flow.

Similarly, by substitution into equation (39),

$$\frac{a_1}{a_0}\frac{\partial\psi}{\partial z_1}\frac{\partial v}{\partial x} + \frac{\partial v}{\partial z_1}\frac{\partial z_1}{\partial z}\left[-\frac{\rho_0}{\rho_1}\left\{\left(\frac{\partial\psi}{\partial x}\right)_{z_1}+\left(\frac{\partial\psi}{\partial z_1}\right)_x\left(\frac{\partial z_1}{\partial x}\right)_y\right\}\right] = \frac{1}{\rho}\frac{\partial}{\partial z}\left[\frac{\mu_0 T}{T_0}\frac{\partial v}{\partial z_1}\frac{a_1\rho}{a_0\rho_0}\right]$$

$$= \frac{\nu_0}{\rho}\frac{p\rho a_1^2}{p_0 a_0^2}\frac{\partial^2 v}{\partial z_1^2}$$

$$= \nu_0\frac{p a_1^2}{p_0 a_0^2}\frac{\partial^2 v}{\partial z_1^2}.$$

Therefore

$$\frac{a_1}{a_0}\frac{\partial\psi}{\partial z_1}\frac{\partial v}{\partial x} - \frac{a_1}{a_0}\frac{\partial v}{\partial z_1}\left\{\frac{\partial\psi}{\partial x}+\frac{\partial\psi}{\partial z_1}\frac{\partial z_1}{\partial x}\right\} = \left(\frac{a_1}{a_0}\right)^{\frac{2\gamma}{\gamma-1}+2}\nu_0\frac{\partial^2 v}{\partial z_1^2}. \quad (53)$$

But

$$\frac{\partial v}{\partial x} = \left\{\left(\frac{\partial v}{\partial z_1}\right)_x\left(\frac{\partial z_1}{\partial x}\right)_y + \left(\frac{\partial v}{\partial x}\right)_{z_1}\right\},$$

hence, cancellation of like terms in equation (53) gives

$$\frac{\partial\psi}{\partial z_1}\frac{\partial v}{\partial x}-\frac{\partial v}{\partial z_1}\frac{\partial\psi}{\partial x}=\left(\frac{a_1}{a_0}\right)^{\frac{3\gamma-1}{\gamma-1}}\nu_0\frac{\partial^2 v}{\partial z_1^2} \quad . \quad . \quad . \quad . \quad (54)$$

and by transformation of the co-ordinate x by equations (44),

$$\frac{\partial\psi}{\partial z_1}\frac{\partial v}{\partial x_1}-\frac{\partial v}{\partial z_1}\frac{\partial\psi}{\partial x_1}=\nu_0\frac{\partial^2 v}{\partial z_1^2} \quad . \quad . \quad . \quad . \quad . \quad (55)$$

The equations of motion corresponding to (52) and (55) in the incompressible case are

$$\left.\begin{aligned}\frac{\partial\psi}{\partial z}\frac{\partial^2\psi}{\partial x\partial z}-\frac{\partial\psi}{\partial x}\frac{\partial^2\psi}{\partial z^2}-\nu\frac{\partial^3\psi}{\partial z^3}&=U\frac{dU}{dx}\\ \frac{\partial\psi}{\partial z}\frac{\partial v}{\partial x}-\frac{\partial\psi}{\partial x}\frac{\partial v}{\partial z}&=\nu\frac{\partial^2 v}{\partial z^2}\end{aligned}\right\} \quad . \quad . \quad . \quad (56)$$

where $u=\partial\psi/\partial z$ and $w=-\partial\psi/\partial x$.

The Natural Frequency of Vibration of Curved Rectangular Plates

P. J. PALMER, Ph.D., M.Sc., D.I.C., A.F.R.Ae.S.

(*Department of Civil Engineering, University of Birmingham*)

Summary: The natural frequency of vibration of curved rectangular plates, with both simply-supported and fixed edges, is evaluated for the fundamental extensional mode. This mode is thought to be applicable when the plates are excited by a uniformly distributed pressure as may occur with a dynamic pressure wave. The natural frequencies corresponding to this mode increase fairly rapidly with the curvature of the plate.

The natural frequency of vibration of the plates when the mode is the fundamental inextensional mode is also considered. The frequency of this mode is higher than that of the extensional mode for small curvatures, but the inextensional mode frequency falls slowly with increase in curvature of the plate. Thus, if the curvature of the plate is sufficiently large, the frequency of the fundamental inextensional mode is lower than that of the extensional mode.

All the frequencies deduced are found by means of the Rayleigh method, in so far as they correspond to initially assumed modes.

1. Introduction

In a recent investigation into the effect of dynamic pressure waves on stressed skin structures, it was found necessary to evaluate the natural frequency of vibration of curved rectangular plates. Very little information appears to have been published on this subject, although as early as 1888 Lamb[1] considered the vibration of curved bars. In 1928, Den Hartog[2] evaluated the natural frequency of vibration of circular arcs when vibrating in both extensional and inextensional modes. The present paper sets out to deal with the natural frequency of vibration of curved rectangular plates while vibrating in fundamental modes.

The natural frequency of vibration of any curved rectangular plate will, of course, depend upon the mode into which it deforms. When designing against dynamic pressure waves, it is thought that, because the load distribution which excites the mode will be approximately uniformly distributed over the plate, the mode produced will be the fundamental symmetrical one in which extension of the middle plane of the plate occurs. Hence, emphasis is placed here upon this type of extensional mode, although an inextensional mode is also investigated. It is quite possible that after the initial excitation, by the pressure wave, the plate may change its mode of vibration, if one of lower frequency exists, but as regards the structural design of the plate and neighbouring structure, it is the mode occurring during the first cycle which is relevant.

Throughout this paper the natural frequencies deduced are those obtained by the Rayleigh solution in so far as they correspond to initially assumed modes, so that the true natural frequencies may be slightly lower than those deduced here.

Originally received April 1953.

[The Aeronautical Quarterly, Vol. V, July 1954]

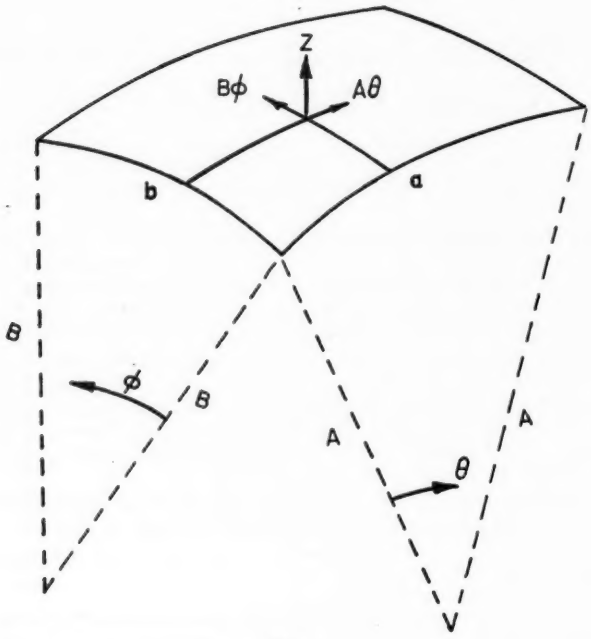

Fig. 1.
Geometry for curved plate.

Notation

a, b	sides of plate
A, B	radii of curvature of plate
$D = E h^3/\{12(1-\nu^2)\}$	
E	modulus of elasticity
f	natural frequency of plate (cycles/sec.)
G	modulus of rigidity
h	thickness of plate
J	amplitude of vibration (time function)
T	kinetic energy
V	potential energy
u, v, w	displacements of plate in the $A\theta$, $B\phi$, and z directions
z	axis normal to plate, outwards from middle plane
ρ	plate density
θ, ϕ	axes of plate

ν Poisson's ratio

$\varepsilon_\theta, \varepsilon_\phi, \gamma_{\theta\phi}$ strain components in plate

$\sigma_\theta, \sigma_\phi, \tau_{\theta\phi}$ stress components in plate

2. The Extensional Mode

This section is concerned with the natural frequency of vibration of a curved plate when the mode is the fundamental symmetrical one, in which extension of the centre plane of the plate takes place.

The case of a flat rectangular plate with simply-supported edges is a classical case and appears in textbooks[3]. The case of a flat plate with fixed edges (fixed as regards position and slope) is not so simple, but the solution using the Rayleigh method has been worked out by Redshaw[4]. The natural frequency of curved rectangular plates with edges either simply-supported or fixed can be evaluated, using the Rayleigh method, as follows.

For a curved rectangular plate, as shown in Fig. 1, with axes in the plate of $A\theta$ and $B\phi$, where A and B are the radii of curvature, the expressions for the strains are, from Timoshenko[5],

$$\left.\begin{aligned} \varepsilon_\theta &= \frac{\partial u}{A\partial\theta} + \frac{w}{A} \\ \varepsilon_\phi &= \frac{\partial v}{B\partial\phi} + \frac{w}{B} \\ \gamma_{\theta\phi} &= \frac{\partial u}{B\partial\phi} + \frac{\partial v}{A\partial\theta} \end{aligned}\right\} \quad . \quad . \quad . \quad . \quad . \quad . \quad (1)$$

where u, v and w are the displacements in the $A\theta$, $B\phi$, and z directions.

The change of curvature in the $A\theta$ direction is

$$\frac{1}{A^2}\left(\frac{\partial u}{\partial\theta} - \frac{\partial^2 w}{\partial\theta^2}\right). \quad . \quad . \quad . \quad . \quad . \quad . \quad (2)$$

For the type of mode being considered, extension of the centre plane of the plate takes place, and points on the centre plane move radially such that u and v are zero. Hence the first term in the expression for the direct strains can be expressed as the distance from the centre of the plate multiplied by the change in curvature. Also, provided that the thickness of the plate is small compared with the radius of curvature, the first term in the expression for change of curvature can be neglected compared with the second.

Thus the expressions for curvature changes are dependent upon w alone, and hence the strains can be expressed in terms of w. This leads to the following expressions for the strains:—

$$\left.\begin{aligned}\varepsilon_\theta &= -\frac{z}{A^2}\frac{\partial^2 w}{\partial\theta^2}+\frac{w}{A}\\ \varepsilon_\phi &= -\frac{z}{B^2}\frac{\partial^2 w}{\partial\phi^2}+\frac{w}{B}\\ \gamma_{\theta\phi} &= -\frac{2z}{AB}\frac{\partial^2 w}{\partial\theta\partial\phi}\end{aligned}\right\} \quad . \quad . \quad . \quad . \quad . \quad . \quad (3)$$

where z is the axis normal to the surface of the plate measured from the middle plane.

In the Rayleigh method, an assumption is made concerning the shape of normal deflection of the plate (*i.e.* the mode). The form taken here for the case of simply-supported edges is

$$w = J\sin\frac{\pi A\theta}{a}\sin\frac{\pi B\phi}{b} \quad . \quad . \quad . \quad . \quad . \quad . \quad (4)$$

where a and b are the lengths of the sides of the plate.

This mode is the simplest form which is symmetrical and which satisfies the boundary conditions

$$\left.\begin{aligned} w &= \frac{\partial^2 w}{\partial\theta^2} = 0 \quad \text{at} \quad \theta = 0 \quad \text{and} \quad a/A\\ w &= \frac{\partial^2 w}{\partial\phi^2} = 0 \quad \text{at} \quad \phi = 0 \quad \text{and} \quad b/B\end{aligned}\right\} \quad . \quad . \quad . \quad (5)$$

It is also that mode which does in fact lead to the exact solution in the case of flat plates.

With fixed or built-in edge supports, the assumed mode will be

$$w = J\,\theta^2\phi^2\,(a - A\theta)^2\,(b - B\phi)^2 \quad . \quad . \quad . \quad . \quad . \quad (6)$$

which is a symmetrical mode, which reduces to that used by Redshaw[4] in the case of flat plates, and which satisfies the boundary conditions given by

$$\left.\begin{aligned} w &= \frac{\partial w}{\partial\theta} = 0 \quad \text{at} \quad \theta = 0 \quad \text{and} \quad a/A\\ w &= \frac{\partial w}{\partial\phi} = 0 \quad \text{at} \quad \phi = 0 \quad \text{and} \quad b/B\end{aligned}\right\} \quad . \quad . \quad . \quad . \quad . \quad (7)$$

The stresses can be expressed in terms of the strains by the following relationships.

$$\left.\begin{aligned}\sigma_\theta &= \frac{E}{(1-\nu^2)}(\varepsilon_\theta + \nu\varepsilon_\phi)\\ \sigma_\phi &= \frac{E}{(1-\nu^2)}(\varepsilon_\phi + \nu\varepsilon_\theta)\\ \tau_{\theta\phi} &= G\gamma_{\theta\phi}.\end{aligned}\right\} \quad . \quad . \quad . \quad . \quad . \quad . \quad (8)$$

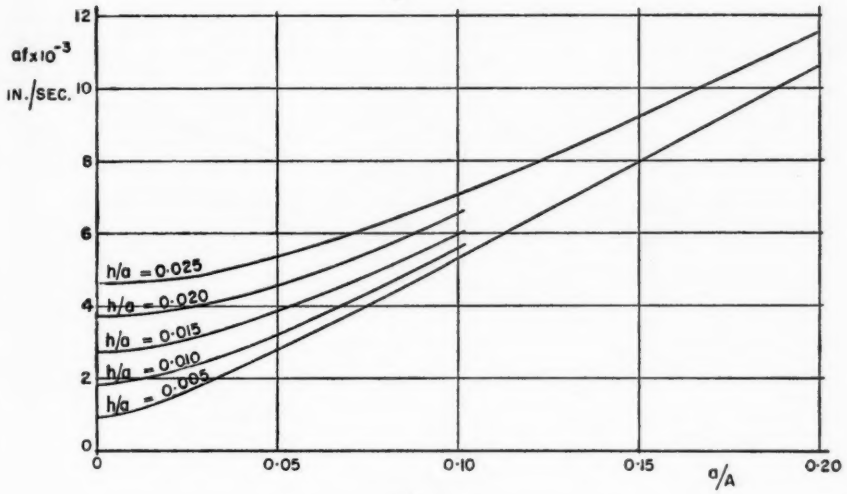

Fig. 2.

Natural frequency of curved square plates. Equal curvature in both directions. Simply-supported edges.

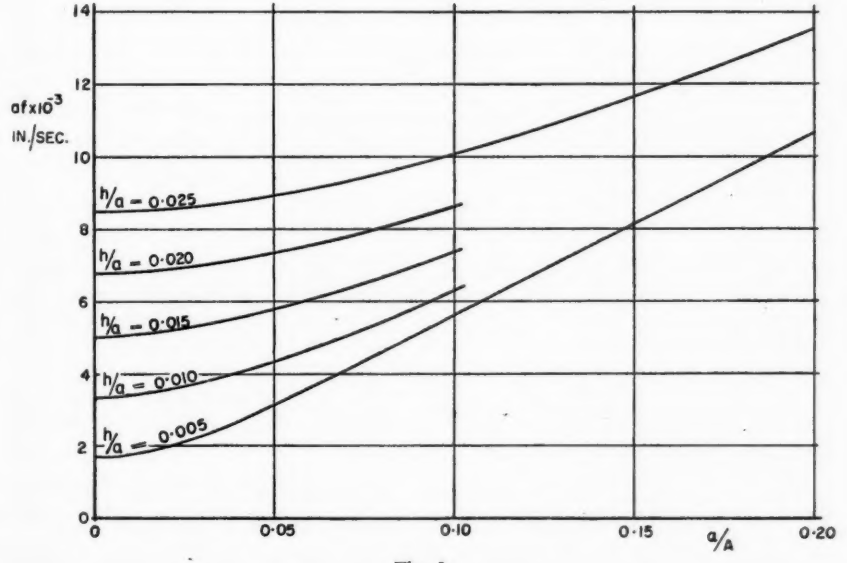

Fig. 3.

Natural frequency of curved square plates. Equal curvature in both directions. Fixed edges.

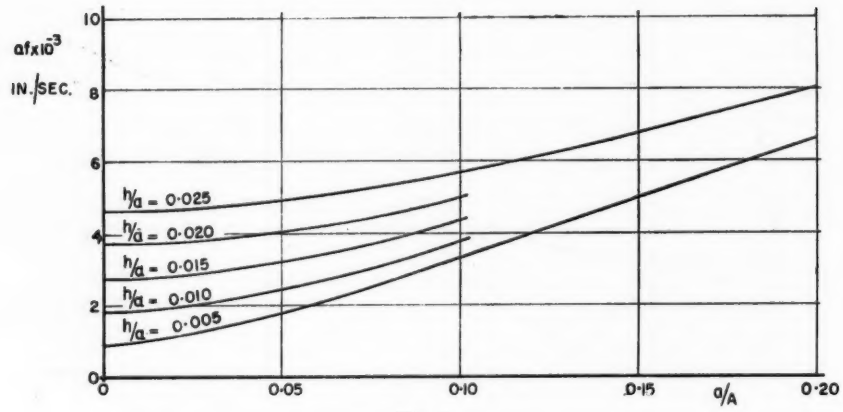

Fig. 4.

Natural frequency of curved square plates. Curved in one direction only. Simply-supported edges.

The potential energy stored in the plate can be obtained from the expression

$$dV = \frac{AB}{2}(\varepsilon_\theta \sigma_\theta + \varepsilon_\phi \sigma_\phi + \gamma_{\theta\phi}\tau_{\theta\phi})\, d\theta\, d\phi\, dz \quad . \quad . \quad . \quad (9)$$

and the kinetic energy, at any time, is given by

$$dT = \tfrac{1}{2}\rho h \dot{w}^2 AB\, d\theta\, d\phi \quad . \quad . \quad . \quad . \quad . \quad . \quad (10)$$

The sum of the potential energy and the kinetic energy will be constant, so that if the total energy is differentiated with respect to time, a differential equation of the following form results.

$$\ddot{J} + CJ = 0. \quad . \quad . \quad . \quad . \quad . \quad . \quad (11)$$

The term J is the amplitude of vibration and, as such, will vary with time, whereas C is independent of time. From this differential equation an expression for the natural frequency of vibration can be deduced. For simply-supported edges, this leads to

$$f = \frac{1}{2\pi}\sqrt{\left(\frac{D}{\rho h}\right)}\sqrt{\left\{\pi^4\left(\frac{1}{a^2}+\frac{1}{b^2}\right)^2 + \frac{12}{h^2}\left(\frac{1}{A^2}+\frac{2\nu}{AB}+\frac{1}{B^2}\right)\right\}} \quad . \quad . \quad (12)$$

and for fixed edges,

$$f = \frac{1}{2\pi}\sqrt{\left(\frac{D}{\rho h}\right)}\sqrt{\left\{72\left(\frac{7}{a^4}+\frac{7}{b^4}+\frac{4}{a^2b^2}\right) + \frac{12}{h^2}\left(\frac{1}{A^2}+\frac{2\nu}{AB}+\frac{1}{B^2}\right)\right\}} \quad (13)$$

These expressions agree with the existing ones for flat plates and it should be noted that, in the limit for large curvatures, the type of edge fixing becomes immaterial.

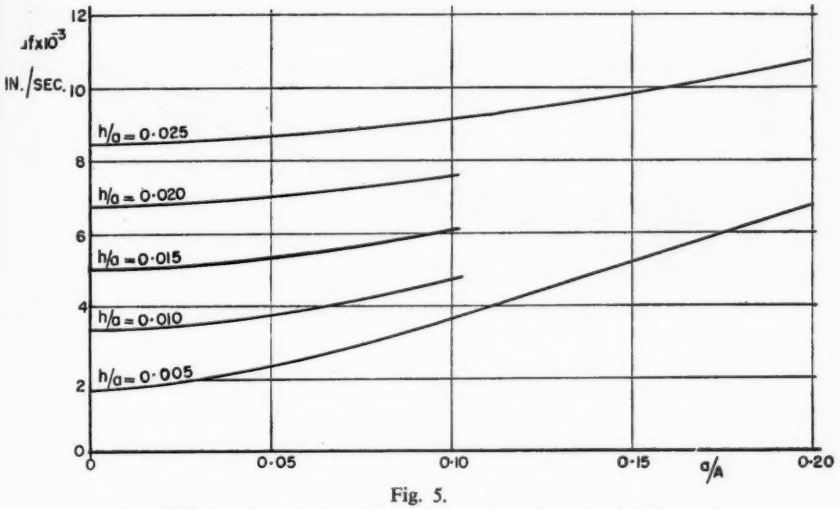

Fig. 5.
Natural frequency of curved square plates. Curved in one direction only. Fixed edges.

The increase of the natural frequency of a plate with curvature is small for very small curvatures, but the increase soon becomes quite large as the curvature increases. Typical results are given for light alloy plates in Figs. 2 to 7. These results are for square plates with equal curvature in both directions, square plates with curvature in one direction alone, and infinitely long rectangular plates curved across the width, all three cases being given for both types of edge support. Here E has been taken as 10×10^6 lb./in.^{2}, ν as 0·3, and ρ as $0{\cdot}1/g$ slugs/in.^{3}

3. The Inextensional Mode

As already mentioned, the natural frequency of the fundamental symmetrical mode, in which extension takes place, is simply that mode which is thought to be the most relevant when designing against dynamic pressure waves. Other modes may occur, notably inextensional modes, in which the natural frequency may be less than that of the extensional mode considered. Here, the fundamental mode cannot be symmetrical, and the fundamental asymmetrical mode, in which no extension of the middle plane of the plate occurs, will be considered. Whereas in the extensional mode the lateral displacements u and v are zero, since the points on the centre plane of the plate deform along radial lines, in the inextensional mode these displacements will now not be zero, but will be such as to cause no extension of the middle plane of the plate.

Thus, the three strain components will be zero in the middle plane of the plate and for the direct strain in the $A\theta$ direction this leads to

$$\frac{\partial u}{\partial \theta} + w = 0 \quad \text{for} \quad z = 0. \qquad (14)$$

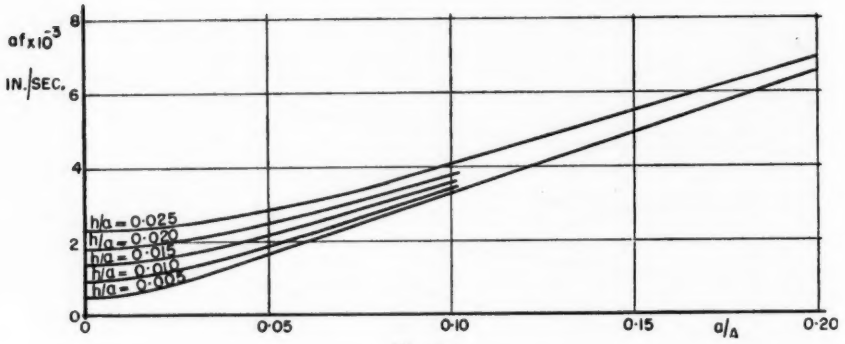

Fig. 6.

Natural frequency of infinitely long rectangular plates, curved across the width. Simply-supported edges.

The change of curvature in the centre plane of the plate, in the $A\theta$ direction, then becomes

$$-\frac{1}{A^2}\left(\frac{\partial^2 w}{\partial\theta^2}+w\right) \qquad . \quad . \quad . \quad . \quad . \quad (15)$$

and the expression for the corresponding strain is

$$\left.\begin{aligned}\varepsilon_\theta &= -\frac{z}{A^2}\left(\frac{\partial^2 w}{\partial\theta^2}+w\right)\\ \text{and similarly}\qquad \varepsilon_\phi &= -\frac{z}{B^2}\left(\frac{\partial^2 w}{\partial\phi^2}+w\right)\end{aligned}\right\} \quad . \quad . \quad . \quad . \quad . \quad (16)$$

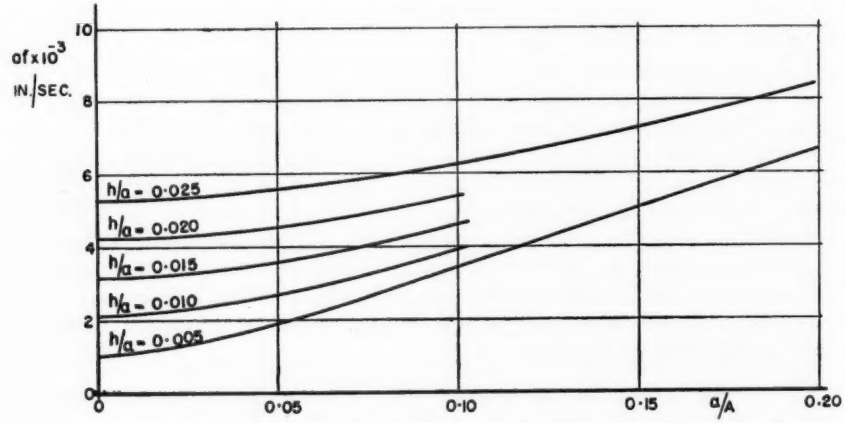

Fig. 7.

Natural frequency of infinitely long rectangular plates, curved across the width. Fixed edges.

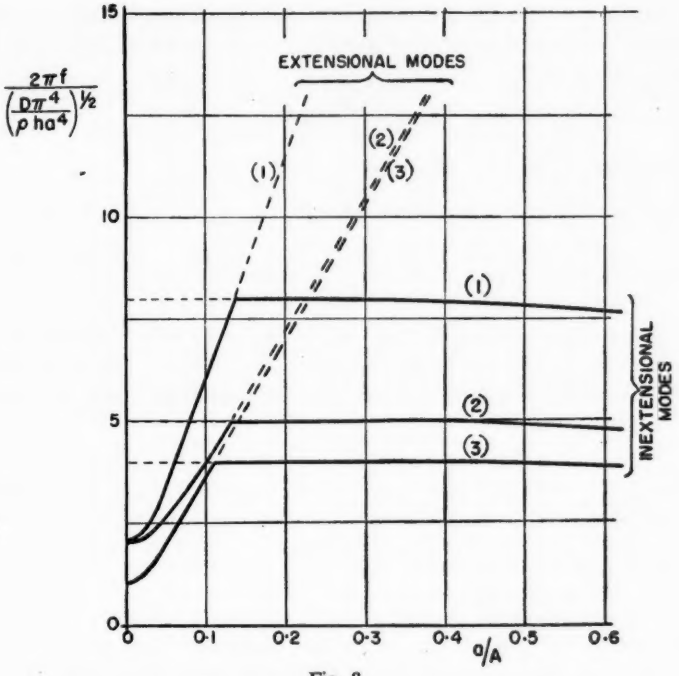

Fig. 8.
Natural frequency in the extensional and inextensional modes.
(Simply-supported edges, $h/a=0{\cdot}01$)
(1) Square plate, equal curvature in both directions.
(2) Square plate, curved in one direction only.
(3) Infinitely long rectangular plate, curved across the width.

The shear strain arising from the bending is given by

$$\gamma_{\theta\phi}=\frac{-z}{AB}\left[2\frac{\partial^2 w}{\partial\theta\partial\phi}+\int\frac{\partial w}{\partial\phi}\,d\theta+\int\frac{\partial w}{\partial\theta}\,d\phi\right] . \quad . \quad . \quad . \quad (17)$$

The lateral displacements u and v can be evaluated from the expressions for the direct strains and these displacements must be such that they are zero at the plate edges in the centre plane. They are

$$u=-\frac{z}{A}\frac{\partial w}{\partial\theta}-\frac{z}{A}\int w d\theta-\int w d\theta+f(\phi) \quad . \quad . \quad . \quad (18)$$

where $f(\phi)$ is such that $u=0$ at $\begin{cases}\theta=0 & \text{and } a/A\\ z=0\end{cases}$

and

$$v=-\frac{z}{B}\frac{\partial w}{\partial\phi}-\frac{z}{B}\int w d\phi-\int w d\phi+g(\theta) \quad . \quad . \quad . \quad (19)$$

where $g(\theta)$ is such that $v=0$ at $\begin{cases}\phi=0 & \text{and } b/B\\ z=0.\end{cases}$

Here again, to obtain the frequency, the Rayleigh method is used and the mode considered for the case of rectangular plates, curved in both directions, with simply-supported edges, is

$$w = J \sin \frac{2\pi A\theta}{a} \sin \frac{2\pi B\phi}{b} \quad . \quad . \quad . \quad . \quad . \quad (20)$$

which is asymmetric in both directions.

This leads to lateral displacements such as

$$u = J \frac{a}{2\pi A} \sin \frac{2\pi B\phi}{b} \left[\frac{z}{A} \left\{ 1 - \left(\frac{2\pi A}{a} \right)^2 \right\} \cos \frac{2\pi A\theta}{a} + \cos \frac{2\pi A\theta}{a} - 1 \right] . \quad (21)$$

The potential and kinetic energies can be evaluated as before and the natural frequency calculated, the main difference now being that the lateral displacements contribute to the total kinetic energy. For the particular case considered the natural frequency is given by

$$f = \frac{1}{2\pi} \sqrt{\left(\frac{D}{\rho h}\right)} \sqrt{\left\{ \frac{(2\pi)^4 \left(\frac{1}{a^2} + \frac{1}{b^2} \right)^2 - 2(2\pi)^2 \left(\frac{1}{a^2 A^2} + \frac{1}{b^2 B^2} + \frac{1}{A^2 b^2} + \frac{1}{a^2 B^2} \right)}{1 + 3\left(\frac{a}{2\pi A} \right)^2 + 3\left(\frac{b}{2\pi B} \right)^2} \right\}}$$

. . . . . (22)

This expression reduces, for flat plates, to the exact solution for the frequency of vibration when the mode is that of the first harmonic. Equation (22) is used to calculate the fundamental inextensional mode frequency only when the plate is curved in both directions. If the plate is curved in only one direction, then the fundamental inextensional mode is asymmetrical in the curved direction and symmetrical in the non-curved direction. All these expressions show that the frequencies fall slightly with increase in curvature. In Fig. 8, the natural frequency of the inextensional mode is compared with that of the extensional mode for the case of plates with simply-supported edges. It can be seen that for small curvatures the extensional mode is of lower frequency than the inextensional mode. As the curvature of the plates increases, the frequency of the extensional mode becomes higher than that of the inextensional mode. The inextensional mode falls slightly with curvature, the fall not becoming appreciable until a/A is about unity.

Similar results would be obtained for plates with fixed edges, when a suitable expression for the inextensional mode, for plates curved in both directions, would be

$$w = J\theta^2\phi^2 (a - 2A\theta)(b - 2B\phi)(a - A\theta)^2 (b - B\phi)^2. \quad . \quad . \quad (23)$$

References

1. Lamb, H. (1888). The Flexture and Vibrations of a Curved Bar. *Proceedings of the London Mathematical Society*, Vol. XIX, p. 365, 1888.
2. Den Hartog, J. P. (1928). The Lowest Natural Frequency of Circular Arcs. *Philosophical Magazine*, Vol. V, p. 400, 1928.
3. Timoshenko, S. (1937). *Vibration Problems in Engineering*. Van Nostrand, p. 421, 1937.
4. Redshaw, S. C. (1942). The Vibration of Flat Plates with Fixed Edges. Boulton Paul Aircraft, Technical Report. Unpublished, 1942.
5. Timoshenko, S. (1940). *Theory of Plates and Shells*. McGraw-Hill, p. 450, 1940.

A Note on the Evaluation of the Supersonic Downwash Integral

B. A. HUNN, B.Sc.
(*lately of Hawker Aircraft Ltd.*)

Summary: To calculate tail loads in flight it is necessary to know the angle of downwash at all points of the tailplane for any given value of wing incidence. Current trends in aircraft design place the tailplane off the plane of the wing. There exist solutions for the downwash in the $z=0$ plane for a delta wing with subsonic leading edges[3, 4]. This note gives a form of integral suitable for numerical evaluation which determines the downwash in the plane of symmetry ($y=0$) of a delta wing with subsonic leading edges. This note also points out an apparent error in Ref. 4 by G. N. Ward and gives a closed form for the downwash at a point whose forward Mach cone totally includes an arrowhead wing with supersonic trailing edges and whose centre line coincides with the axis of the cone.

The procedure adopted is the use of standard elliptic function theory, which in certain cases can eliminate a large amount of tedious analysis. The problem has already been dealt with in general terms in Ref. 2, although the particular solution for the arrowhead wing is not included.

1. Introduction

In the determination of loads on an aircraft and the estimation of its response in manoeuvre it is necessary to know the aerodynamic loads on the wings and tailplane. The calculation of wing loads has been treated exhaustively by numerous authors. The determination of the aerodynamic influence of the wings on the tailplane loads, however, has not been dealt with to such an extent, largely because of the complexity of the integrals involved.

The problem discussed here is that of downwash induced in the plane of symmetry of the aircraft when the wings have straight leading edges whose sweepback is such that they are subsonic in a supersonic main stream. In the first part, the downwash due to a delta wing at incidence, having a simple triangular plan form, is considered. In the second part the case of swallow tail wings is discussed.

Notation

$B^2 = M^2 - 1$	
$\mathrm{E}(k), \mathrm{E}$	complete elliptic integrals of the second kind
$\mathrm{E}'(\lambda) = \mathrm{E}([1-\lambda^2]^{\frac{1}{2}})$	
$\mathrm{E}(\phi, k), \mathrm{E}(\alpha, k)$	incomplete elliptic integrals of the second kind
c	maximum chord of the delta wing
c_0, c_1	*see* after equation (29)
d	distance of point $(x, 0, z)$ behind trailing edge

Originally received October 1952.
[The Aeronautical Quarterly, Vol. V, July 1954]

$K(k), K$	complete elliptic integrals of the first kind
$F(\phi, k)$	incomplete elliptic integral of the first kind
k	modulus of the elliptic functions
$\left.\begin{matrix}\mathrm{sn}(u,k)\\ \mathrm{cn}(u,k)\\ \mathrm{dn}(u,k)\end{matrix}\right\}$	Jacobian elliptic functions
$\Theta(u)$	Jacobi's Theta function
$Z(u)$	Jacobi's Zeta function
$k' = (1-k^2)^{\frac{1}{2}}$	
$\alpha = \mathrm{sn}^{-1}(i\nu/k)$	
α_0	wing incidence
$\alpha', \beta', \gamma', \delta$	*see* equation (37)
β	*see* equation (31)
$\eta = \tan\gamma$	
η_1	*see* after equation (29)
γ	semi-vertex angle of the wing
$\nu = \eta x'/z$	
$\varphi = \tan^{-1}\{(1/Bz)[(x-x')^2 - B^2z^2]^{\frac{1}{2}}\}$	
$\lambda = B\eta$	
ϕ	velocity potential of disturbance
w	z-component of the disturbance velocity
(x, y, z)	Cartesian co-ordinates
y', u, x', t	variables of integration
$K'(k) = K([1-k^2]^{\frac{1}{2}})$	
Ξ	*see* equation (19)
$\mathscr{F}\int$	finite part of the integral (*see* Ref. 1)

2. Theory

Using a right-handed system of Cartesian co-ordinates (x, y, z) such that x is measured positively in the direction of the undisturbed stream and z is positive downwards, with the origin at the vertex of the delta wing, the solution of the linearised lift problem which satisfies

$$B^2\frac{\partial^2\phi}{\partial x^2} - \frac{\partial^2\phi}{\partial y^2} - \frac{\partial^2\phi}{\partial z^2} = 0 \qquad . \quad . \quad . \quad . \quad (1)$$

where $\nabla\phi = \mathbf{u}$, the disturbance velocity vector,

and $B^2 = M^2 - 1$,

is given by

$$\left(\frac{\partial\phi}{\partial x}\right)_{z=0+} = \frac{\alpha_0 U\eta^2}{E'(\lambda)}\frac{x}{[\eta^2x^2 - y^2]^{\frac{1}{2}}} \qquad . \quad . \quad . \quad . \quad (2)$$

on the wing, and the subsonic leading edge condition $B\eta < 1$ is satisfied.

It has been shown[4] that the velocity potential at any point inside the Mach cone from the origin is given by

$$\phi(x,y,z)=\frac{1}{\pi}\iint\frac{\partial\phi}{\partial x'}(x',y',0+)\frac{z(x-x')\,dx'dy'}{[(y-y')^2+z^2][(x-x')^2-B^2(y-y')^2-B^2z^2]^{\frac{1}{2}}} \qquad (3)$$

where the integration extends only over the wing in the forward Mach cone from (x,y,z) where (2) holds, since in the vortex sheet of the wake $\partial\phi/\partial x=0$. To facilitate the analysis it will be assumed that $\phi(x,0,z)$ is required and furthermore that the delta wing is totally within the forward Mach cone from $(x,0,z)$, *i.e.*

$$[(x-c)^2-B^2z^2]^{\frac{1}{2}}>\lambda c,$$

where c is the maximum chord of the wing. The problem now is the evaluation of

$$\phi(x,0,z)=\frac{z_0U\eta^2}{\pi E'(\lambda)}\int_0^c z(x-x')\,x'dx'\int_{-\eta x'}^{\eta x'}\frac{dy'}{[y'^2+z^2][(x-x')^2-B^2y'^2-B^2z^2]^{\frac{1}{2}}[\eta^2x'^2-y'^2]^{\frac{1}{2}}}. \qquad (4)$$

For this the following substitution is made:—

$$y'=\eta x'\,\mathrm{sn}\,(u,k) \qquad (5)$$

$$k^2=\frac{\lambda^2x'^2}{(x-x')^2-B^2z^2} \qquad (6)$$

$\mathrm{sn}\,u$ being a Jacobian elliptic function. Writing $\nu=\eta x'/z$, we get

$$\phi(x,0,z)=\frac{2\,z_0U\eta^2}{\pi E'(\lambda)}\int_0^c\frac{z(x-x')\,dx'}{\lambda}\int_0^K\frac{k^2}{z^2}\frac{du}{(1+\nu^2\mathrm{sn}^2u)}. \qquad (7)$$

The integral in u can be evaluated[5] and gives the form

$$\int_0^K\frac{du}{1-k^2\mathrm{sn}^2\alpha\,\mathrm{sn}^2u}=K(k)+k^2\mathrm{sn}^2\alpha\int_0^K\frac{\mathrm{sn}^2u\,du}{(1-k^2\mathrm{sn}^2\alpha\,\mathrm{sn}^2u)} \qquad (8)$$

where $k^2\mathrm{sn}^2\alpha=-\nu^2$.

This can be written[5] finally as

$$K(k)+\frac{\mathrm{sn}\,\alpha}{\mathrm{cn}\,\alpha\,\mathrm{dn}\,\alpha}\left\{\tfrac{1}{2}\log_e\frac{\Theta(K-\alpha)}{\Theta(K+\alpha)}+K(k)\,Z(\alpha)\right\} \qquad (9)$$

where Θ and Z are Jacobi's Theta and Zeta functions respectively.

However, $$\mathrm{dn}\,(u,k)=\frac{\Theta\,(0)\,\Theta\,(\mathrm{K}+u)}{\Theta\,(\mathrm{K})\,\Theta\,(u)} \quad . \quad . \quad . \quad . \quad . \quad (10)$$

and since dn u and $\Theta\,(u)$ are even functions of u, (9) reduces to

$$\mathrm{K}\,(k)\left\{1+\frac{\mathrm{sn}\,\alpha}{\mathrm{cn}\,\alpha\,\mathrm{dn}\,\alpha}\mathrm{Z}\,(\alpha)\right\} \quad . \quad . \quad . \quad . \quad (11)$$

To evaluate the downwash velocity w, we use the result

$$w=\frac{\partial\phi}{\partial z} \quad . \quad . \quad . \quad . \quad . \quad . \quad (12)$$

so that $$w=\frac{2\,\alpha_0 U\eta^2}{\pi\mathrm{E}'\,(\lambda)}\frac{\partial}{\partial z}\int_0^c\frac{\mathrm{K}\,(k)\,k\,(x-x')}{z\lambda}\left\{1+\frac{\mathrm{sn}\,\alpha}{\mathrm{cn}\,\alpha\,\mathrm{dn}\,\alpha}\mathrm{Z}\,(\alpha)\right\}dx'. \quad . \quad (13)$$

Splitting this integral into two parts and using the definition of $\mathrm{Z}\,(\alpha)$ and sn α gives

$$\mathrm{I}_1=\frac{2\,\alpha_0 U\eta^2}{\pi\mathrm{E}'\,(\lambda)}\frac{\partial}{\partial z}\int_0^c\frac{(x-x')}{\lambda z}\mathrm{K}\,(k)\,k\,dx' \quad . \quad . \quad . \quad (14)$$

$$\mathrm{I}_2=\frac{2\,\alpha_0 U\eta^2}{\pi\mathrm{E}'\,(\lambda)}\frac{\partial}{\partial z}\int_0^c\frac{ix'}{[\eta^2x'^2+z^2]^{\frac{1}{2}}}\{\mathrm{KE}\,(\alpha,k)-\alpha\mathrm{E}\}\,dx' \quad . \quad (15)$$

using the definition of $\mathrm{KZ}\,(\alpha)$ and the fact that $k\,\mathrm{sn}\,\alpha=i\nu$.

To perform the differentiation, the following results are easily obtainable:—

(*i*) $$\frac{\partial\mathrm{E}}{\partial z}(\alpha,k)=-\frac{i\,(x-x')}{\lambda x'z^2}[\eta^2x'^2+z^2]^{\frac{1}{2}}\,k+\frac{k^2z}{\eta^2x'^2}\{E\,(\alpha,k)-(1-k^2)\,\alpha-k^2\alpha\}$$

(*ii*) $$\frac{\partial\alpha}{\partial z}=-\frac{i\,(x-x')\,k}{[\eta^2x'^2+z^2]^{\frac{1}{2}}}\frac{1}{\lambda x'}+\frac{zk^2}{\eta^2x'^2\,(1-k^2)}\left\{\mathrm{E}\,(\alpha,k)-(1-k^2)\,\alpha-\frac{k^2\mathrm{sn}\,\alpha\,\mathrm{cn}\,\alpha}{\mathrm{dn}\,\alpha}\right\}$$

(*iii*) $$\frac{\partial\mathrm{K}}{\partial z}=zk^2\frac{\{\mathrm{E}-(1-k^2)\,\mathrm{K}\}}{\eta^2x'^2\,(1-k^2)}$$

(*iv*) $$\frac{\partial\mathrm{E}}{\partial z}=-\frac{zk^2\,(\mathrm{K}-\mathrm{E})}{\eta^2x'^2}$$

(*v*) $$\frac{\partial k}{\partial z}=\frac{zk^3}{\eta^2x'^2}.$$

Substituting these results where necessary in (14) and (15) and adding, the final result is obtained:—

$$w=\frac{2\alpha_0 U\eta^2}{\pi \mathrm{E}'(\lambda)}\left\{\int_0^c \frac{k\mathrm{E}(x-x')}{\lambda}\left(\frac{k^2}{(1-k^2)\eta^2x'^2}-\frac{1}{(1-k^2)(\eta^2x'^2+z^2)}\right)dx'-\right.$$

$$\left.-\int_0^c \frac{ix'z}{[\eta^2x'^2+z^2]^{3/2}}\Big(\mathrm{KE}(\alpha,k)-\alpha\mathrm{E}\Big)dx'\right\} \quad . \quad . \quad . \quad (16)$$

However,

$$i\Big(\mathrm{KE}(\alpha,k)-\alpha\mathrm{E}\Big)=\mathrm{KF}(\varphi,k')+\mathrm{KE}(\varphi,k')+\mathrm{EF}(\varphi,k')-\frac{\mathrm{K}\lambda x'}{zk(x-x')}[\eta^2x'^2+z^2]^{\frac{1}{2}} \quad (17)$$

where
$$\varphi=\tan^{-1}\left\{\frac{[(x-x')^2-B^2z^2]^{\frac{1}{2}}}{Bz}\right\} \quad . \quad . \quad . \quad . \quad (18)$$

Thus on combining equations (16), (17), (18), and using standard tables of incomplete elliptic integrals it is now possible to evaluate the integrands at as many values of x' as are necessary to obtain a good approximation to the integral.

It is interesting at this stage to pursue the limiting process of letting z tend to zero. Writing

$$\Xi=-\mathrm{KF}(\varphi,k')+\mathrm{KE}(\varphi,k')+\mathrm{EF}(\varphi,k') \quad . \quad . \quad . \quad (19)$$

we consider

$$\lim_{z\to 0}\frac{2\alpha_0 U\eta^2}{\pi \mathrm{E}'(\lambda)}\int_0^c\left\{\frac{-\Xi x'z}{[\eta^2x'^2+z^2]^{3/2}}+\frac{\mathrm{K}\lambda x'^2}{k(x-x')(\eta^2x'^2+z^2)}+\right.$$

$$\left.+\frac{\mathrm{E}(x-x')k}{\lambda(1-k^2)}\left(\frac{k^2}{\eta^2x'^2}-\frac{1}{\eta^2x'^2+z^2}\right)\right\}dx'. \quad . \quad . \quad (20)$$

Now
$$\lim_{z\to 0}k(x-x')=\lambda x' \quad . \quad . \quad . \quad . \quad . \quad (21)$$

and
$$\lim_{z\to 0}\Xi=\mathrm{KE}'+\mathrm{EK}'-\mathrm{KK}'=\pi/2. \quad . \quad . \quad . \quad . \quad (22)$$

But

$$\int_0^c\frac{\Xi x'z}{[\eta^2x'^2+z^2]^{3/2}}dx'=\left[\frac{\Xi z}{\eta^2[\eta^2x'^2+z^2]^{\frac{1}{2}}}\right]_0^c-\int_0^c\frac{z}{\eta^2[\eta^2x'^2+z^2]^{\frac{1}{2}}}\frac{\partial\Xi}{\partial x'}dx' \quad . \quad (23)$$

and, since Ξ is a finite continuous function of x' within the range, it may be shown that the limit of the integral is simply

$$\lim_{z\to 0}\int_0^c\frac{\Xi x'z\,dx'}{[\eta^2x'^2+z^2]^{3/2}}=\pi/(2\eta^2). \quad . \quad . \quad . \quad . \quad (24)$$

Thus
$$w(x,0,0)=\frac{2\,\alpha_0 U\eta^2}{\pi E'(\lambda)}\left\{\int_0^c \frac{K-E}{\eta^2 x'}\,dx'-\pi/(2\,\eta^2)\right\} \quad . \quad . \quad . \quad (25)$$

But since
$$k=\frac{\lambda x'}{(x-x')}; \qquad dk=\frac{x\lambda}{(x-x')^2}dx',$$

then
$$w(x,0,0)=\frac{2\,\alpha_0 U}{\pi E'(\lambda)}\left\{\int_0^{\lambda c/d}\frac{\lambda\,(K-E)}{k\,(\lambda+k)}\,dk-\pi/2\right\} \quad . \quad . \quad . \quad (26)$$

$$=\frac{2\,\alpha_0 U}{\pi E'(\lambda)}\left\{E\left(\frac{\lambda c}{d}\right)+\int_0^{\lambda c/d}\left(\frac{K-E}{k+\lambda}\right)dk\right\}, \quad . \quad (27)$$

These are the results obtained in Ref. 3 and quoted finally in Ref. 4. The results obtained in Ref. 4 equation (12), will be seen to be incorrect, which is apparently due to a fallacious statement in equation (11).

Consider the downwash due to a swept wing, when the pressure on the lower surface is given, using

$$\frac{\partial\phi}{\partial x}=\frac{\alpha_0 U\eta^2}{\pi E'}\frac{x}{[\eta^2x^2-y^2]^{\frac{1}{2}}} \quad . \quad . \quad . \quad . \quad . \quad (28)$$

In order that this may be true we have to make the following restrictions on the wing:—

(*i*) The trailing edges must be supersonic with respect to the trailing edge apex Mach cone for the speed range considered.

(*ii*) The tip must be pointed, so that in fact swallow tail wings are considered.

Now the downwash will be obtained from the integral as shown in (3), with the bounds of integration modified. However, it is equally simple to complete the delta by filling in the triangular wake region whose vertices are the two wing tips and the trailing edge apex and, using the downwash formula for complete delta wings, to obtain that due to the swallow tail wing by subtracting the downwash due to this triangular wake as if it were wing.

Thus if we require the downwash at $A\,(x,0,z)$ behind the swallow tail we have to evaluate the correction term

$$w'=\frac{2\,\alpha_0 U\eta^2}{\pi E'(\lambda)}\frac{\partial}{\partial z}\int_{c_1}^{c_0} z\,(x-x')\,x'dx'\int_0^{\eta_1(x'-c_1)}\frac{dy'}{[y'^2+z^2]\,[(x-x')^2-By'^2-B^2z^2]^{\frac{1}{2}}[\eta^2x'^2-y'^2]^{\frac{1}{2}}}$$

$$. \quad . \quad . \quad . \quad . \quad . \quad . \quad . \quad . \quad . \quad (29)$$

where $x=c_1$ defines the trailing edge apex,

$x=c_0$ defines the value of x at the tips,

and $\eta_1=\cot\Lambda_T$,

the sweepback of the trailing edge being Λ_T. There is one other condition which has to be accounted for, namely that involving the amount of the wing included in the forward Mach cone from A. We shall consider here the algebraically more simple case when the whole wing can be included. This can be expressed by the condition

$$\eta x' < (1/B)(x-x'), \quad \text{when} \quad z=0. \qquad (30)$$

We use the same substitution as before and introduce β by the definition

$$\eta x' \operatorname{sn}\beta = \eta_1 (x'-c_1). \qquad (31)$$

The general solution in the xz-plane has been obtained, but owing to its algebraic complexity it has not been included. The correction term for the downwash at $A(x,0,0)$ due to an arrowhead wing is found to be, using a result from Ref. 1,

$$\frac{w'}{U} = \frac{2\alpha_0}{\pi \mathrm{E}'(\lambda)} \mathscr{F} \int_{S'} \mathscr{F} \int \frac{dx'du}{x' \operatorname{sn}^2(u,k)}, \quad k=\frac{\lambda x'}{x-x'} \qquad (32)$$

where S' denotes the triangular cut-out, and $\mathscr{F}$ indicates "finite part." We have:—

$$\mathscr{F} \int_0^\beta \frac{du}{\operatorname{sn}^2(u,k)} = \mathrm{F}(\varphi,k) - \mathrm{E}(\varphi,k) - \frac{\operatorname{cn}\beta \operatorname{dn}\beta}{\operatorname{sn}\beta} \qquad (33)$$

so that

$$\frac{w'}{U} = \frac{2\alpha_0}{\pi \mathrm{E}'(\lambda)} \mathscr{F} \int_{c_1}^{c_0} \left[\frac{\mathrm{F}(\varphi,k)-\mathrm{E}(\varphi,k)}{x'} - \frac{\operatorname{cn}\beta \operatorname{dn}\beta}{x' \operatorname{sn}\beta} \right] dx' \qquad (34)$$

where

$$\operatorname{sn}\beta = \frac{\eta_1 (x'-c_1)}{\eta x'} = \sin\varphi. \qquad (35)$$

Hence the final result for the arrowhead wing totally included in the forward Mach cone from A is

$$\frac{w}{U} = \frac{2\alpha_0}{\pi \mathrm{E}'(\lambda)} \left\{ \int_0^c \left(\frac{\mathrm{K}-\mathrm{E}}{x'} \right) dx' - \pi/2 - \int_{c_1}^{c_0} \frac{\mathrm{F}(\varphi,k)-\mathrm{E}(\varphi,k)}{x'} dx' + \right.$$

$$\left. + \mathscr{F} \int_{c_1}^{c_0} \frac{[\eta^2 x'^2 - \eta_1^2 (x'-c_1)^2]^{\frac{1}{2}} [(x-x')^2 - \lambda_1^2 (x'-c_1)^2]^{\frac{1}{2}}}{x' \eta_1 (x'-c_1)(x-x')} dx' \right\}. \qquad (36)$$

The last integral whose principal part is required can be evaluated by the standard process of writing

$$t^2 = \left(\frac{\beta' - \delta}{\alpha' - \delta}\right)\left(\frac{x' - \alpha'}{x' - \beta'}\right); \quad k^2 = \left(\frac{\alpha' - \delta}{\alpha' - \gamma'}\right)\left(\frac{\beta' - \gamma'}{\beta' - \delta}\right) \quad . \quad . \quad (37)$$

where α', β', γ', δ are the roots of $\left(\eta^2 x'^2 - \eta_1^2 (x' - c_1)^2\right)\left((x - x')^2 - \lambda_1^2 (x' - c_1)^2\right)$ in x'.

References

1. Lomax, H., Heaslet, M. A. and Fuller, F. B. (1951). Integrals and Integral Equations in Linearized Wing Theory. N.A.C.A. Report 1054, 1951.
2. Lomax, H., Sluder, L. and Heaslet, M. A. (1950). The Calculation of Downwash Behind Supersonic Wings with an Application to Triangular Planforms. N.A.C.A. Report 957, 1950.
3. Robinson, A. and Hunter-Tod, J. H. (1947). Bound and Trailing Vortices in the Linearized Theory of Supersonic Flow and the Downwash in the Wake of a Delta Wing. R. & M. 2409, 1947.
4. Ward, G. N. (1949). Calculation of Downwash Behind a Supersonic Wing. *The Aeronautical Quarterly*, Vol. 1, May 1949.
5. Copson, E. T. (1935). *The Theory of Functions of a Complex Variable*. Oxford University Press, 1935.

The Design of Thin Finite Wings in Incompressible Flow

G. J. HANCOCK, B.Sc.
(Department of Mathematics, Sheffield University)

Summary: A method is developed for designing thin finite wings with prescribed lift distributions. Particular attention is given to wings which, at a certain optimum angle of incidence, have zero loading along the whole leading edge. It is suggested that such a wing will have a greater range of lift coefficient for low drag than other wings with the same plan form.

On the basis of the linearised theory a formula, relating the wing surface to the pressure distribution over the surface, is deduced which differs from the usual potential relationship by avoiding the difficulty of the non-uniform convergence with respect to the normal distance away from the wing surface singularities. The surface integral which is developed includes a regular singularity and a definite limiting process.

Three examples have been worked out in which the condition of smooth flow at the leading edge is satisfied.

In the first example, the pressure distribution of a rectangular aerofoil is assumed to be elliptic in the chordwise direction and parabolic in the spanwise direction. The reverse pressure distribution (parabolic chordwise, elliptic spanwise) is considered in the second example over the same rectangular aerofoil. Thirdly a pressure distribution is prescribed over a swept-back wing.

1. Introduction

Of the two basic aims of aerodynamic calculation, namely

(*i*) to determine the pressure distribution in flow past an obstacle of given shape

(*ii*) to determine an obstacle shape having a given pressure distribution,

only problem (*i*) has received great attention in problems of flow over three-dimensional wings at low Mach numbers, although both problems have been extensively treated for two-dimensional aerofoils.

As is well known, the symmetrical part of the pressure distribution, resulting from the fairing of the wing, is much easier to determine than the anti-symmetrical part, resulting from camber and angle of incidence. This is because, to the first-order approximation used, the symmetrical part of the potential functions is determined from a boundary condition which is of the same type all over the plane which contains the wing; while the boundary condition for the anti-symmetrical part is of mixed type. This is unfortunate because the lift distribution is what is most needed.

For problem (*ii*) the situation is reversed. The easier problem here is the determination of the shape of the central surface such that the lift at a given angle of incidence is distributed in a given manner. (This is the extension to three dimensions of Goldstein's theory[1] of the design of camber lines.)

Originally received July 1952.
[The Aeronautical Quarterly, Vol. V, July 1954]

No work seems to have been done on problem (*ii*), while theoretical work on lift distribution on wings has consisted either of accurate computations taking many months, or approximate methods with restricted ranges of application. The labour of the accurate methods has been justified as helping to indicate more precisely the ranges of application of the approximate methods.

Now if, instead, some exact solutions are found by solving the design problem (*ii*), with (as will be seen) far less labour, these can equally be used as a testing ground for approximate methods of the solution of problem (*i*). This in itself makes the development of the necessary technique worth while. In addition, theoretical knowledge of what sort of camber distribution and twist may be expected to produce specific effects on lift distribution, particularly for unconventional plan forms, is almost certainly worth having.

The question now arises—what sort of lift distribution should be aimed at? In this first paper on the subject the author has decided to concentrate on designing a central surface such that each section of the wing achieves its optimum incidence simultaneously, namely at the cruising lift coefficient. If a suitable fairing were added, this wing would have quite a range of values of C_L about this optimum C_L, in which the drag might be expected to be low. By optimum incidence is meant the condition of zero loading at the leading edge so that there would be no tendency to breakdown even if no fairing whatever were put onto the central surface.

The general problem of determining the shape of the central surface from the lift distribution is solved in Sections 2 and 3. In this work the fairing is neglected and the problem reduces to the determination of the shape of an (infinitely) thin wing from its assumed pressure distribution. The difficulty of the simplest formal approach, in leading to a result containing improper integrals, is avoided by an extension of the method devised by Ursell[2] for the determination of the pressure distribution on symmetrical wings at zero lift. As a result the determination of a wing surface for a prescribed pressure distribution becomes a direct double integration.

In Sections 4, 5 and 6 three examples satisfying the condition mentioned, of zero wing loading at the leading edge for a prescribed value of C_L, are designed.

Notation

x, y, z	rectangular Cartesian co-ordinates
$z=\zeta(x, y)$	equation of the wing surface
$x=l(y)$ $x=t(y)$	equations of the leading and trailing edges of the wing surface on the plane $z=0$
V	velocity of the main stream
(u, v, w)	disturbance velocity at point (x, y, z)
$p(x, y, z)$	disturbance pressure
$\phi(x, y, z)$	velocity potential
S_W	wing projection on plane $z=0$

S_T	trailing vortex projection on plane $z=0$
$\mathbf{R}$	vector $X, Y, 0$
$\mathbf{r}$	vector x, y, z
S_P	small surface in space $z>0$ around $(X, Y, 0)$
C_P	curve of intersection of S_P with xy-plane
S_L	small surface in space $z>0$ around $x=l(y)$
S_{+s}	small surface in space $z>0$ around $y=+s$
S_{-s}	small surface in space $z>0$ around $y=-s$
S'	large hemisphere in space $z>0$ centre $(X, Y, 0)$
$S_W'+S_T'$	the plane surface S_W+S_T excluding the interior of curve C_P and the regions of the perimeter, $x=l(y)$ and $\|y\|=s$
ε, a	sides of the rectangle C_P parallel to x- and y-axes respectively
P_L	limiting operation $\varepsilon \longrightarrow 0$ first and $a \longrightarrow 0$ secondly
α	angle of incidence

2. Mathematical Formulation

The incompressible flow past a thin wing at a small angle of incidence is now considered. As shown in Fig. 1, the origin of the rectangular Cartesian axes is taken at the mid-point of the centre chord of the wing. The equation of the wing surface is defined as $z=\zeta(x, y)$, and the equations of the leading and trailing edges of the projection of the wing surface on the plane $z=0$ are $x=l(y)$ and $x=t(y)$ respectively.

If V is the velocity of the main stream at infinity, and (u, v, w) is the disturbance

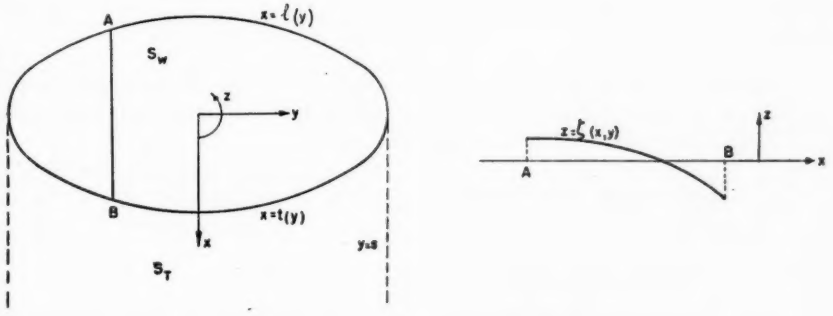

Fig. 1.
Plan and elevation of a thin finite wing.

velocity at the point (x, y, z) due to the presence of the aerofoil in the stream, the linearised equations of motion are

$$\left.\begin{aligned} V\frac{\partial u}{\partial x} &= -\frac{1}{\rho}\frac{\partial p}{\partial x} \\ V\frac{\partial v}{\partial x} &= -\frac{1}{\rho}\frac{\partial p}{\partial y} \\ V\frac{\partial w}{\partial x} &= -\frac{1}{\rho}\frac{\partial p}{\partial z} \end{aligned}\right\} \quad . \quad . \quad . \quad . \quad . \quad . \quad (1)$$

The equation of continuity becomes

$$\frac{\partial u}{\partial x} + \frac{\partial v}{\partial y} + \frac{\partial w}{\partial z} = 0. \quad . \quad . \quad . \quad . \quad (2)$$

The problem is to determine the relationship between a doublet distribution over the projection of the wing and trailing vortex sheet on the plane $z=0$, and the shape of the wing surface. The conditions to be satisfied are that smooth flow exists over the wing surface and that the pressure is continuous over the vortex sheet. The condition of adjacent flow states that on the wing plan form

$$\frac{w(x, y, 0)}{V} = \frac{\partial \zeta(x, y)}{\partial x} \quad . \quad . \quad . \quad . \quad . \quad (3)$$

where $w(x, y, 0)$ is calculated from the doublet distribution.

The flow outside the region of the doublet distribution is irrotational, therefore a velocity potential ϕ exists such that

$$u = -\frac{\partial \phi}{\partial x}, \quad v = -\frac{\partial \phi}{\partial y}, \quad w = -\frac{\partial \phi}{\partial z}.$$

Then the problem reduces to the determination of the discontinuity in ϕ over a certain surface in the xy-plane with the condition that $(\partial\phi/\partial z)_{z=0}$ satisfies equation (3).

Denoting the wing projection on the xy-plane by S_W and the projection on the xy-plane of the trailing strip from $x=t(y)$ to $x=+\infty$, $(|y| \leqslant s)$ by S_T, the following boundary conditions are to be satisfied.

(*i*) Since ϕ is an odd function of z, *i.e.* $\phi(x, y, z) = -\phi(x, y, -z)$,

$$\phi = u = v = 0.$$

w remains finite on the plane $z=0$ outside $S_W + S_T$.

(*ii*) Over S_W; the discontinuity $\phi_{z=+0} - \phi_{z=-0}$ is a function of x and y; therefore discontinuities in u, v exist. Since $\partial\phi/\partial z$ is an even function of x, w is finite, satisfying equation (3).

(*iii*) Over S_T, since there is no pressure discontinuity across S_T, the velocity u must be continuous and therefore $u=0$, hence $\phi_{z=+0}-\phi_{z=-0}$ is a function of y only.

(*iv*) It is assumed in accordance with the usual linearised theory that in the region of the perimeters of S_W+S_T,

$$\phi_{z=+0}-\phi_{z=-0}=O(\delta^{\frac{1}{2}})$$

when δ is the distance from the particular perimeter, either near the leading edge $x=l(y)$ or the lines $|y|=s$.

Thus $$u_{z=+0}-u_{z=-0}=O(\delta^{-\frac{1}{2}}), \qquad v_{z=+0}-v_{z=-0}=O(\delta^{-\frac{1}{2}})$$

and $$\frac{\partial}{\partial x}(u_{z=+0}-u_{z=-0})=O(\delta^{-3/2}), \quad \frac{\partial}{\partial y}(v_{z=+0}-v_{z=-0})=O(\delta^{-3/2})$$

near the boundaries mentioned.

3. Application of Green's Theorem

Following Ursell[2] a point $P(X, Y)$ on S_W is considered. The point $(X, Y, 0)$ is denoted by the vector $\mathbf{R}$ and (x, y, z) by $\mathbf{r}$. A small surface S_P is constructed around P in the space $z>0$, cutting the plane $z=+0$ in a curve C_P. Green's theorem is to be applied to the two harmonic functions w and $1/(\mathbf{R}-\mathbf{r})$ over the region bounded by the plane $z=+0$ (excluding singularities) and a large hemisphere above $z=0$.

Since $$\frac{\partial w}{\partial z}=-\left(\frac{\partial u}{\partial x}+\frac{\partial v}{\partial y}\right)=O(\delta^{-3/2}),$$

from boundary condition (4), in the region of any perimeters of S_W+S_T, it is necessary to construct small cylindrical surfaces S_L, S_s, S_{-s} around these perimeters as shown in Fig. 2.

If S' is a large hemisphere, centre $(X, Y, 0)$,

$$\iint\left(w\frac{\partial}{\partial n}\frac{1}{|\mathbf{R}-\mathbf{r}|}-\frac{1}{|\mathbf{R}-\mathbf{r}|}\frac{\partial w}{\partial n}\right)dS=0 \quad . \quad . \quad . \quad (4)$$

where the integration is over the surface comprising S', S_P, S_L, S_{+s}, S_{-s}, and the plane $z=+0$ exterior to C_P which completes the closed surface. If the radius of S' tends to infinity, the integral over S' vanishes and equation (4) reduces to

$$\iint\left(w\frac{\partial}{\partial n}\frac{1}{|\mathbf{R}-\mathbf{r}|}-\frac{1}{|\mathbf{R}-\mathbf{r}|}\frac{\partial w}{\partial n}\right)dS=0 \quad . \quad . \quad . \quad (5)$$

the integral being taken over the surface $S_L+S_{+s}+S_{-s}+S_P+S_W'+S_T'$ where $S_W'+S_T'$ denotes the surface S_W+S_T for $z=+0$, excluding the interior of C_P and

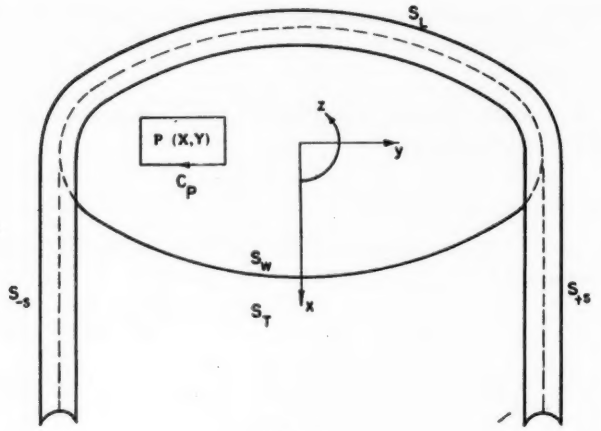

Fig. 2.
Surfaces around the singularities.

excluding the regions of the perimeters. Each of the integrals of (5) will now be considered separately.

(*a*) First the integral over $z=+0$ will be considered.

$$\iint_{S_W'+S_T'} \left(w \frac{\partial}{\partial n} \frac{1}{|\mathbf{R}-\mathbf{r}|} - \frac{1}{|\mathbf{R}-\mathbf{r}|} \frac{\partial w}{\partial n} \right) dS = \iint_{S_W'+S_T'} \frac{1}{[(x-X)^2+(y-Y)^2]^{\frac{1}{2}}} \frac{\partial w}{\partial z} dxdy$$

since $\partial/\partial n \equiv -\partial/\partial z$.

Replacing $\partial w/\partial z$ by $-(\partial u/\partial x + \partial v/\partial y)$ and integrating by parts,

$$\iint_{S_W'+S_T'} \frac{1}{[(x-X)^2+(y-Y)^2]^{\frac{1}{2}}} \frac{\partial w}{\partial z} dxdy =$$

$$- \int_{-s}^{+s} \left[\frac{u(x,y)}{[(x-X)^2+(y-Y)^2]^{\frac{1}{2}}} \right]_{x=l(y)}^{x=\infty} dy - \int_{l(0)}^{\infty} \left[\frac{u(x,y)}{[(x-X)^2+(y-Y)^2]^{\frac{1}{2}}} \right]_{y=-s}^{+s} dx -$$

$$- \oint_{C_P} \frac{u(x,y)\cos\theta + v(x,y)\sin\theta}{[(x-X)^2+(y-Y)^2]^{\frac{1}{2}}} d\xi - \iint_{S_W'+S_T'} \frac{u(x,y)(x-X)+v(x,y)(y-Y)}{[(x-X)^2+(y-Y)^2]^{3/2}} dxdy \quad . \qquad (6)$$

where $dx/d\xi = \sin\theta$, $dy/d\xi = \cos\theta$ around the curve C_P.

(*b*) Secondly the integral over S_P is considered, where C_P is taken as a rectangle of sides 2ε, $2a$ parallel to the x- and y-axes respectively. S_P is now taken as a semi-cylinder of length $2a$, radius ε. The integral over the surface S_P then reduces

to $2\pi w(X, Y)$ if the limiting process $\varepsilon \longrightarrow 0$ is applied first and the process $a \longrightarrow 0$ afterwards.

(*c*) Finally the integrals over S_L, $S_{-\varepsilon}$, $S_{+\varepsilon}$ are evaluated, as these surfaces tend to zero and may be shown to cancel out the line integrals over the perimeter of $S_W + S_T$ in equation (6).

Hence from (*a*), (*b*) and (*c*), equation (5) reduces to

$$2\pi w(X, Y) - P_L \left\{ \oint_{C_P} \frac{u(x, y)\cos\theta + v(x, y)\sin\theta}{[(x-X)^2 + (y-Y)^2]^{\frac{1}{2}}} d\xi + \right.$$

$$\left. + \int\int_{S_W + S_T} \frac{(x-X)\,u(x, y) + (y-Y)\,v(x, y)}{[(x-X)^2 + (y-Y)^2]^{3/2}} dxdy \right\} = 0$$

where P_L denotes the operation $\lim \varepsilon \longrightarrow 0$ first and $\lim a \longrightarrow 0$ afterwards.

Since the line integral vanishes in the application of P_L,

$$2\pi w(X, Y) = P_L \left\{ \int\int_{S_W + S_T} \frac{(x-X)\,u(x, y) + (y-Y)\,v(x, y)}{[(x-X)^2 + (y-Y)^2]^{3/2}} dxdy \right\} \quad . \quad . \quad . \quad (7)$$

4. Determination of a Wing Surface of a Rectangular Wing of Aspect Ratio 2 with Optimum Angle of Incidence along the Span

It was explained in Section 1 that it is desirable to design a wing possessing smooth flow along the leading edge. This is performed by prescribing a pressure distribution which vanishes like $\delta^{\frac{1}{2}}$ (where δ is the small distance from the edge) at the leading edge as well as the trailing edge. By the relationship of equation (1), the velocities u and v on the surface $S_W + S_T$ are determined; therefore on substitution in the right hand side of equation (7) the velocity $w(X, Y)$ is determined, and hence $\zeta(x, y)$ is known by equation (3).

To simplify some initial calculations, the case of a rectangular wing is considered, where the plan form is given by $-1 \leqslant x \leqslant +1$, $-s \leqslant y \leqslant +s$.

The pressure distribution is assumed to be

$$p = -\rho V^2 K\alpha (1-x^2)^{\frac{1}{2}} \left(1 - \frac{y^2}{s^2}\right)$$

where K is a constant such that the angle of incidence at the centre section is α.

Hence by equation (1),

$$\frac{u(x,y)}{V} = K\alpha(1-x^2)^{\frac{1}{2}}\left(1-\frac{y^2}{s^2}\right) \qquad \text{on} \quad S_W$$

$$= 0 \qquad \text{on} \quad S_T$$

$$\frac{v(x,y)}{V} = -K\alpha\frac{y}{s^2}\left[x(1-x^2)^{\frac{1}{2}} + \sin^{-1}x + \frac{\pi}{2}\right] \qquad \text{on} \quad S_W$$

$$= -K\alpha\frac{\pi}{s^2} \qquad \text{on} \quad S_T.$$

On substitution in equation (7),

$$\frac{2\pi w(X,Y)}{VK\alpha} =$$

$$P_L\left\{\iint_{S_W}\frac{(x-X)(1-x^2)^{\frac{1}{2}}(1-y^2/s^2)-(y/s^2)(y-Y)[x(1-x^2)^{\frac{1}{2}}+\sin^{-1}x+\pi/2]dxdy}{[(x-X)^2+(y-Y)^2]^{3/2}} + \right.$$

$$\left. + \iint_{S_T} -\frac{y\pi}{s^2}\frac{y-Y}{[(y-Y)^2+(x-X)^2]^{3/2}}\,dxdy\right\}.$$

In this formula $s=2$ is taken. The integration with respect to y is performed; then the integration with respect to x is calculated numerically. The values of $w(X,Y)/(VK\alpha)$ are given in Table I, and the graph of the surface $z=\zeta(x,y)$ is shown in Fig. 3. It must be remembered that equation (3) gives only the relationship between $\partial\zeta/\partial x$ and $w(x,y,0)$ due to the assumptions of the linearised theory, and therefore in the determination of $\zeta(x,y)$ an arbitrary function of y has to be assumed. In this example the assumption is made that the leading edge lies on the xy-plane.

From the graph in Fig. 3 the value of K is 3·6.

TABLE I

VALUES OF $w(X,Y)/(VK\alpha)$

	$Y=$ 0·0	0·5	1·0	1·5	2·0
$X=-1{\cdot}00$	0·673	0·637	0·625	0·407	0·147
$-0{\cdot}75$	0·436	0·434	0·359	0·318	0·083
$-0{\cdot}50$	0·178	0·177	0·160	0·201	0·285
$-0{\cdot}25$	$-0{\cdot}063$	$-0{\cdot}054$	$-0{\cdot}006$	0·107	0·324
$-0{\cdot}00$	$-0{\cdot}289$	$-0{\cdot}262$	$-0{\cdot}164$	0·042	0·348
$+0{\cdot}25$	$-0{\cdot}468$	$-0{\cdot}434$	$-0{\cdot}284$	0·007	0·426
$+0{\cdot}50$	$-0{\cdot}643$	$-0{\cdot}590$	$-0{\cdot}386$	$-0{\cdot}009$	0·521
$+0{\cdot}75$	$-0{\cdot}788$	$-0{\cdot}714$	$-0{\cdot}476$	$-0{\cdot}021$	0·625
$+1{\cdot}00$	$-0{\cdot}948$	$-0{\cdot}760$	$-0{\cdot}701$	$-0{\cdot}041$	0·730

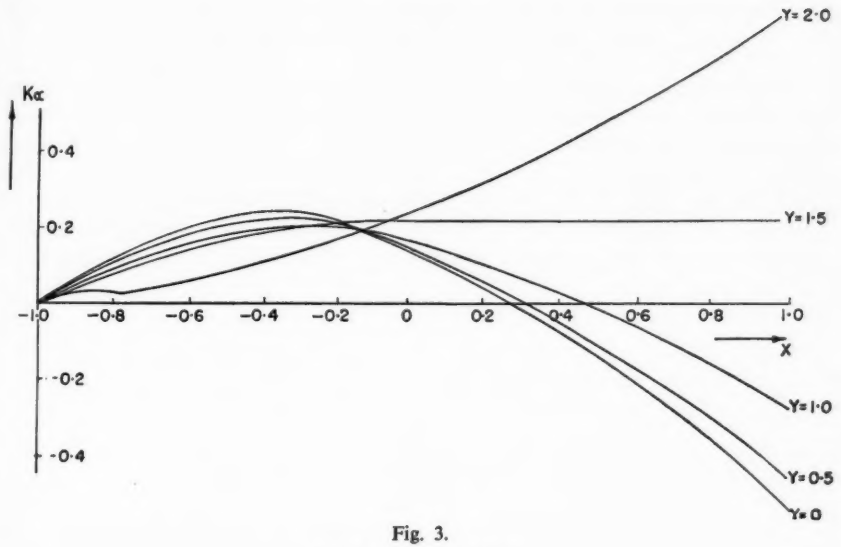

Fig. 3.

Wing Surface $z = \zeta(x, y)$.

Rectangular wing with optimum incidence across the span.

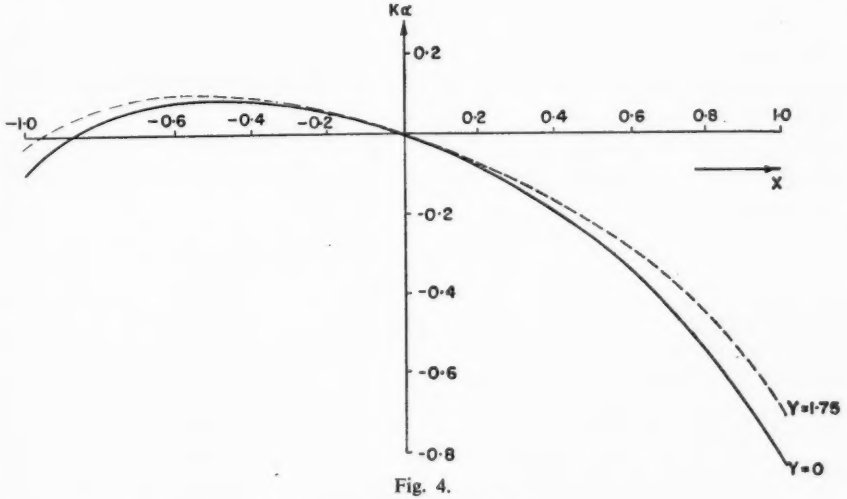

Fig. 4.

Wing surface $z = \zeta(x, y)$.

Rectangular wing with elliptic circulation distribution.

5. Determination of a Rectangular Wing of Aspect Ratio 2 with Prescribed Elliptic Circulation Distribution

In the last example a pressure distribution is prescribed which satisfies the flow conditions in the chordwise direction but which states that the circulation distribution in the spanwise direction is parabolic. The wing which satisfies this pressure distribution is seen to have a total twist in the region of the wing tips. To show that this twist is due to the assumption of the parabolic distribution of circulation, an example is now worked out for an elliptic circulation distribution, together with a parabolic chordwise distribution to simplify the calculations.

The prescribed pressure distribution is therefore taken to be

$$p = -\rho V^2 K\alpha (1-x^2)\left(1-\frac{y^2}{s^2}\right)^{\frac{1}{2}}$$

Hence

$$\frac{u}{V} = K\alpha (1-x^2)\left(1-\frac{y^2}{s^2}\right)^{\frac{1}{2}} \quad \text{on} \quad S_W$$

$$= 0 \quad \text{on} \quad S_T$$

$$\frac{v}{V} = \frac{-yK\alpha}{s^2(1-y^2/s^2)^{\frac{1}{2}}}\left(x-\frac{x^3}{3}+\frac{2}{3}\right) \quad \text{on} \quad S_W$$

$$= \frac{-4yK\alpha}{3s^2(1-y^2/s^2)^{\frac{1}{2}}} \quad \text{on} \quad S_T.$$

The values of $w/(VK\alpha)$ have been computed at the two sections $Y=0$, $Y=1{\cdot}75$ and are given in Table II. The graph of this wing is indicated in Fig. 4, where $K=2{\cdot}7$.

It is seen that, to achieve a uniform pressure distribution in the spanwise direction, no twist is needed and only a slight reduction of camber at the tips should be applied.

TABLE II

VALUES OF $w/(VK\alpha)$

	$Y=$ 0	1·75
$X=1{\cdot}0$	−1·60	−1·40
0·5	−0·80	−0·70
0·0	−0·33	−0·33
−0·5	−0·05	+0·05
−1·0	+0·90	+0·70

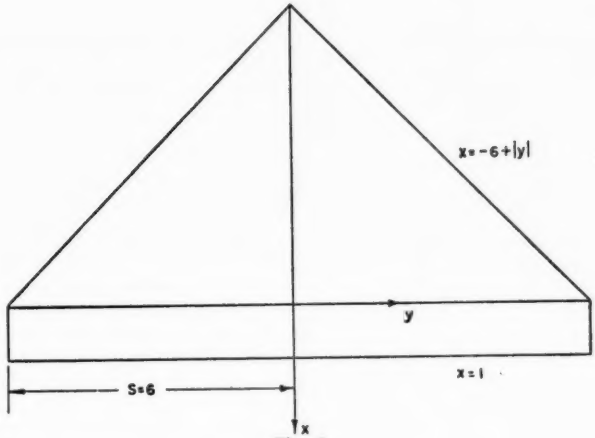

Fig. 5.
Delta wing.

6. Determination of a 45° Swept-back Wing

The greatest interest is in the application of the design criterion to swept-back wings. One example is now worked out, the delta wing whose equations of the leading and trailing edges are

$$x = -6 + |y|$$
$$\text{and } x - 1 = 0,$$

and whose span $s=6$. This wing is shown in Fig. 5.

The prescribed pressure distribution will be assumed to possess the properties previously stated (*i.e.* elliptic circulation, smooth flow at the leading and trailing edges), together with the property that the derivatives of the pressure across the centre line of the aerofoil are continuous. Therefore the pressure distribution is taken to be

$$p=\rho V^2 \frac{Kz}{49}\left(x+6+\frac{|y|}{2}\right)\left[(x+6-|y|)(1-x)\left(1-\frac{y^2}{36}\right)\right]^{\frac{1}{2}}$$

TABLE III

VALUES OF $w/(VKz)$

	$Y=$ 0	2	4
$X=-6$	+0·04		
$X=-4$	−0·03	+0·10	
$X=-2$	−0·18	−0·01	+0·15
$X=-1$	−0·50	−0·25	+0·05
$X=+1$	−0·80	−0·55	−0·35

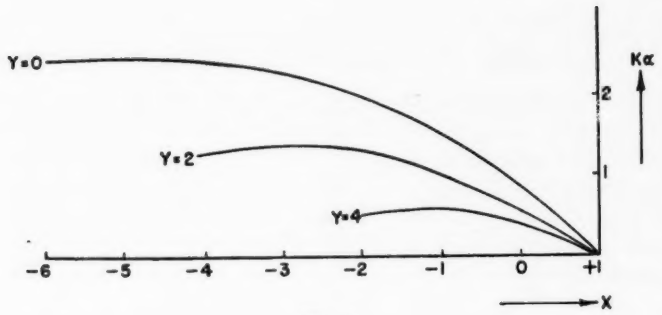

Fig. 6.
Wing surface $z=\zeta(x, y)$. Delta wing.

Therefore

$$\frac{u}{V}=\frac{K\alpha}{49}\left(x+6+\frac{|y|}{2}\right)\left[(x+6-|y|)(1-x)\left(1-\frac{y^2}{36}\right)\right]^{\frac{1}{2}} \quad \text{on } S_W$$

$$=0 \quad \text{on } S_T$$

$$\frac{v}{V}=\frac{-yK\alpha}{1764(1-y^2/36)^{\frac{1}{2}}}\left\{\left[\frac{1}{8}(7-|y|)^2(7+2|y|)+\frac{27}{2}\left(1-\frac{y^2}{36}\right)(7-|y|)\right]\times\right.$$

$$\times\left[\sin^{-1}\frac{x+\frac{1}{2}(5-|y|)}{\frac{1}{2}(7-|y|)}+\frac{\pi}{2}\right]+\left[\frac{(7+2|y|)}{2}\left(x+\frac{1}{2}(5-|y|)\right)+27\left(1-\frac{y^2}{36}\right)\right]\times$$

$$\left.\times[(1-x)(x+6-|y|)]^{\frac{1}{2}}-\frac{2}{3}[(1-x)(x+6-|y|)]^{3/2}\right\} \quad \text{on } S_W$$

$$=\frac{-y\pi K\alpha}{1764(1-y^2/36)^{\frac{1}{2}}}\left\{\frac{1}{8}(7-|y|)^2(7+2|y|)+\frac{27}{2}\left(1-\frac{y^2}{36}\right)(7-|y|)\right\} \quad \text{on } S_T.$$

The values of $w/(VK\alpha)$ have been computed at the three sections $Y=0$, 2, 4 and are given in Table III. In the graph of the wing (Fig. 6) the assumption has been made that the trailing edge lies on the xy-plane, and it is seen that $K=2{\cdot}8$.

The wing seems to have only a slight constant twist in the spanwise direction, as the camber at each section increases. It will be noticed that the leading point of the delta wing is hardly curved at all to meet the oncoming fluid.

Acknowledgment

The author wishes to thank Dr. M. Holt for his many useful suggestions in connection with this paper.

References
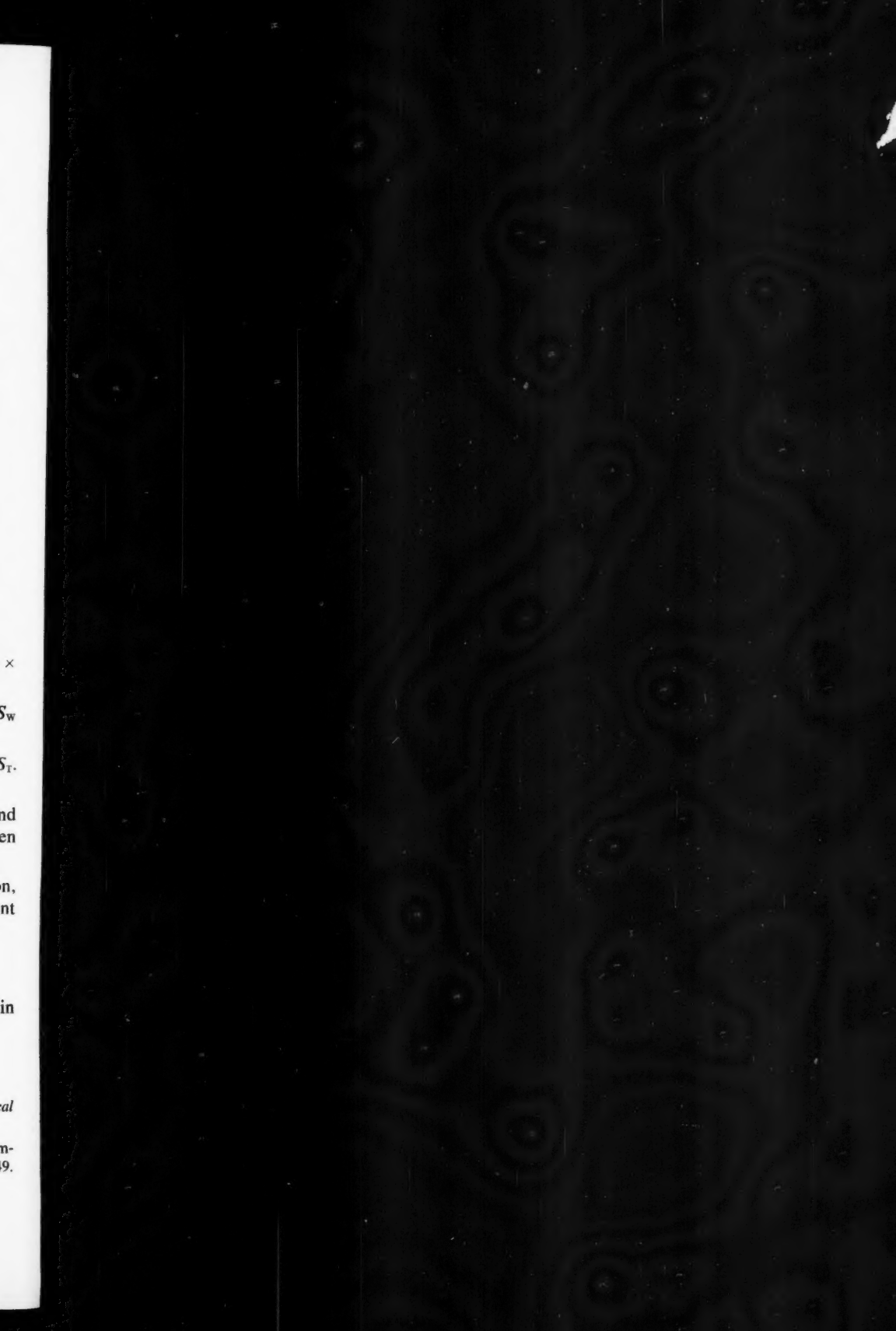
1. Goldstein, S. (1948). Low Drag and Suction Aerofoils. *Journal of the Aeronautical Sciences*, Vol. 15, April 1948.
2. Ursell, F. (1949). Notes on the Linear Theory of Incompressible Flow Around Symmetrical Swept-Back Wings at Zero Lift. *The Aeronautical Quarterly*, Vol. I, May 1949.